ASTRONOMY & ASTROPHYSICS
SUPPLEMENT SERIES

FEBRUARY **1995**, PAGE 293

Astron. Astrophys. Suppl. Ser. **109**, 293-312 (1995)

Heterochromatic extinction. I. Dependence of interstellar extinction on stellar temperature, surface gravity, and metallicity*

E.K. Grebel[1,2] and Wm J. Roberts[3]

[1] European Southern Observatory, Casilla 19001, Santiago 19, Chile
[2] Sternwarte der Universität Bonn, Auf dem Hügel 71, D-53121 Bonn, Germany, grebel@astro.uni-bonn.de
[3] Space Telescope Science Institute, 3700 San Martin Drive, Baltimore, MD 21218, U.S.A., roberts@stsci.edu

Received April 15; accepted May 9, 1994

Abstract. — Techniques used to remove atmospheric extinction cannot be used for interstellar extinction, because objects can be observed at only a single extinction, which varies from object to object. The interstellar extinction is thus unknowable without the use of prior information about the object. In this paper we show how to apply such knowledge in the case of normal stars. Using standard passbands, an accepted average optical interstellar extinction law, and Kurucz flux tables, we derive useful colour-dependent interstellar extinction relations for synthetic versions of two widely used sets of broad band photometric passbands, Johnson-Cousins $UBVRI$ and Washington CMT_1T_2. For the Washington system, we define a new internal reddening system. For bands blueward of 500 nm in either photometric system the reddenings for main sequence stars and evolved stars are quite different, and even can be non-linear as a function of temperature colour. These corrections are important for the correct characterisation of the intrinsic reddening properties of interstellar dust, for fitting isochrones accurately, for determining stellar metallicities, for obtaining correct standard reddenings for reddened galactic clusters, and indeed for the determination of basic stellar parameters for single stars such as $T_{\rm eff}$ and $M_{\rm bol}$. To make the reddenings to different objects comparable, we standardise the reddening on that of a solar metallicity main sequence star of $T_{\rm eff}$ = 17 000 K (B3–4 V). The functional dependence of the extinction curves on abundance is not as important in the Johnson-Cousins as in the Washington system. We compute new theoretical reddening vectors in both systems, and evaluate the size of the nonlinearity with extinction (Forbes effect).

Key words: ISM: dust, extinction — techniques: photometric — stars: fundamental parameters

1. Introduction

The light of a star can be considered to be a probe of the optical properties of the medium it traverses. We may want to study the medium or to get rid of its effects. Though it is a necessary tool in astronomical studies, broadband photometry has serious deficiencies as the measuring instrument. One of the generally recognised complications of using a broadband photometric system is the colour dependence of atmospheric and interstellar extinctions in the individual filter bands. The theory of this dependence is more fully developed in the case of atmospheric extinction (see Young 1992a, 1994 for new developments and a summary of history). In this paper we apply a practical technique, avoiding moment theory (e.g., Young 1992a) and vector space theory (Young 1994), but depending on some prior knowledge of the stellar spectrum, which we have applied successfully to atmospheric extinction transformations (Roberts & Grebel 1995a: Paper II).

The nonlinearity of the interstellar reddening trajectory in the $U-B$, $B-V$ two colour diagram was first noted by Blanco (1956, 1957) and Hiltner & Johnson (1956), and received a careful analysis by Wildey (1963) with the best data and methods available at the time. Blanco considered what is called the Forbes effect in atmospheric extinction (Sect. 4), while Hiltner, Johnson, and Wildey considered primarily the dependence of interstellar extinction on colour. In the first case the absorption is nonlinear in a single band because the absorption is dependent on wavelength, in the second because the absorption in the

Send offprint requests to: E.K. Grebel, Sternwarte Bonn
*All colour dependent extinctions and their fit coefficients for main sequence stars, giants, and supergiants at [Fe/H] = 0.5, 0.0, −1.0, and −2.0 dex in the $UBVRI$ and Washington filters are available in electronic form in the SIMBAD database at CDS (see Editorial in A&AS 1994, Vol. 103, No. 1).

bands of the colour indices depends on the colour of the star.

Wildey provided practical prescriptions for dereddening, and suggested the possible importance of other factors such as abundance on the extinction. The nonlinearity (i.e., curved reddening trajectory) studied by Wildey could not be distinguished from simultaneous changes in the $U-B$ and $B-V$ reddenings caused by linear variations with intrinsic $(B-V)_0$ (or temperature). We show in this paper that *nonlinear* variations with temperature colour in the extinction of individual bandspasses can be quite important, as also can be variations with surface gravity and metallicity. We rely on no formal analyses, but present only the phenomenology of the colour corrections. We will call the dependence of the extinction on the parameters $T_{\rm eff}$, $\log g$, [Fe/H] of the spectrum of the stellar probe the *generalised Wildey extinction.*

The colour dependence of interstellar extinction for the UBV and Geneva broadband (and three intermediate bands) systems has been considered using formal methods in Golay (1974), who cautions the observer against relying on unverified linear transformations, which is all that most current dereddening and magnitude transformation programs do. However, practical help in making the appropriate corrections was not provided.

We undertook this study in order to be able to make consistent interstellar reddening colour transformations in our program that fits synthetic isochrones in several colour magnitude diagrams (CMDs) simultaneously. That is, it finds the most likely population parameters by simultaneously rating a set of isochrones differing in metallicity and age, of distance moduli, and of reddenings against CMDs in all independent colour indices (Grebel & Roberts 1994) using robust maximum likelihood estimation in order to determine reddening in addition to the usual parameters of the stellar population: age and metallicity.

The ability to deredden correctly all independent colour indices in a set of photometric images of a stellar population is very important for the reliable measurement of the parameters of the population. Variations by colour and thus temperature in the $U-B$ and $C-M$ reddening in particular complicate the fits to the upper main sequence (MS) of young clusters. For reddened open clusters, if one does not properly consider the variation in relative reddening for cool giants, one cannot derive correct broadband photometric reddenings or metallicities, and will have additional difficulties estimating age and distance modulus. Metallicities are commonly determined photometrically from calibrations of morphological parameters of, e.g., the colour of the giant branch in a CMD or by the distribution of stars in a calibrated two colour diagram (TCD, e.g., Geisler et al. 1991; Grebel et al. 1994c,d). For both of these methods, and particularly the latter, accurate dereddenings are essential in at least two colour indices, one of which must involve blue filters ($U-B$, $B-V$, or $C-M$).

A common error is to deredden Cepheids by the same amount at all phases of the light curve, or even all the same regardless of colour. In BVR they are less reddened near minimum light than they are near maximum. Thus the usual procedure systematically underestimates the amplitudes of these variables and overestimates the mean luminosity, and this error correlates with the amount of reddening, systematically affecting the derived relations among these quantities. Cepheids should be correctly dereddened as a function of temperature and surface gravity at each phase, also taking account of the actual metallicity of the Cepheid. Since the calibrating Galactic Cepheids are fairly reddened, these variations may affect systematically the calibrations of the distance scale. This problem seems to be a different issue from that raised recently by Gould (1994), in which systematic variations in measured distance modulus as a function of Cepheid metallicity were found in two external galaxies.

Another common error is to deredden the blue horizontal branch (BHB) of a globular cluster the same amount as the RGB. The reddening in $B-V$ of the BHB is 20% greater than that of the RGB, so the differences of the intrinsic colours computed would be in error by this fraction of the reddening. This variation must be considered when studying reddened disk and bulge globular clusters, else the measured morphological parameters of the CMDs will be systematically wrong.

We have gained much insight from the photometric investigations that have been pursued in atmospheric extinction by Young, Manfroid, and their coworkers. That problem is not altogether dissimilar to the problem of interstellar extinction, which is considered here from a point of view different from these authors. There is one fundamental respect in which the problems of interstellar and atmospheric extinction differ: one can observe a star at only a single interstellar extinction, so to properly remove that extinction, some assumption about the spectrum of the star is unavoidable. Young has argued (e.g., 1992a, 1992b) that if one can observe a star at different airmasses in a well-sampled photometric system, in the Shannon sense (no such system exists at the moment), in principle one need not use any prior information about the spectrum of the star or other target in order to successfully transform away the extinction. *Thus for removing interstellar extinction some method like ours must be used, while for atmospheric extinction a broader range of techniques is possible.* We will leave most discussion of atmospheric extinction to Paper II. Prior information about the spectrum of the star of course does not necessarily imply a prior spectroscopic analysis of a given star but may encompass more general information as can be inferred from CCD photometry of stellar aggregates where reasonable assumptions about the majority of individual

stars can be made based on their position in the colour-magnitude diagram.

Our work in this paper is confined to synthetic forms of the two broadband systems in widest use, Johnson-Cousins $UBVRI$ and Washington CMT_1T_2, the two systems in which almost all of our photometry has been taken. *Strictly speaking, our analysis applies to the $UBVRI$ standard passbands provided to us by M. Bessell, and not to the Johnson UBV standard system and its various RI extensions.* The RI passbands provided by Bessell are the Cousins R_CI_C passbands. However, neither differences among the standard systems, such as northern and southern Johnson UBV, Kron or Cousins RI, etc., nor their differences from the true extra-atmospheric magnitudes have a significant effect on our results. We usually will refer to the Johnson-Cousins system as $UBVRI$, and sometimes will refer to the Washington system as WCS for Washington Canterna System, after the astronomy department where it originated and its principal architect (Canterna 1976). The passbands used for the two synthetic systems are shown in Fig. 1 of Paper II. The blue set $UBV+CM$ and the atmospheric extinction spectrum we have adopted, converted to transmission, is displayed in more detail in Fig. 1.

We have chosen T_2 instead of T_1 as the principal magnitude for WCS in this study for several reasons.

- T_1 is poorly designed according to the fundamental work of Young (1992a), being too asymmetric, so should be replaced;
- T_1 has the smallest bandwidth, and T_2 is much more sensitive for the cool stars for which Washington was designed;
- Cardelli et al. (1989) have shown that the wavelength range covered by T_2 (Fig. 1 Paper II) is the bluest for which the extinction does not seem affected by variations in the physical properties of the dust, as evidenced by variations in R, that is, it is nearly independent of the line of sight. Hence this band makes a superior reference band to V or to any other Washington band.

After describing our methods and results, we show how to apply them and discuss their significance for the study of both dust and stars. *We can provide no guidance or treatment for the dereddening of broadband photometry of non-stellar objects, stars with emission lines, or unresolved binaries, or stars that are peculiar in other aspects (such as chemically peculiar stars), which cannot be done correctly without detailed knowledge of the spectrum of the object.*

2. Method

There are only three ingredients to our method: (1) standard photometric passbands, or response functions, (2) an interstellar extinction law, and (3) a library of synthetic stellar spectra. The details of our results depend on the accuracy of all ingredients, but the general conclusions do not.

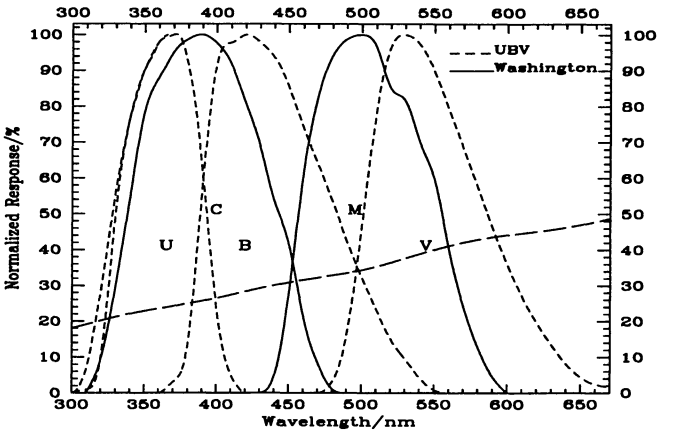

Fig. 1. Five normalised crucial broadband filter passbands, UBV and CM, useful for measuring metallicity, surface gravity, and reddening. The dashed curve shows the Scheffer interstellar extinction law as fit with cubic splines

Our $UBVRI$ passbands were obtained from Bessell (1992) after we had difficulty reproducing correct colours from Kurucz synthetic spectra using previously published passbands. We have validated these passbands both against the measured colours of stars with atmospheric parameters derived from high dispersion spectra (Roberts & Grebel 1995b), and against our own $UBVRI$ and Washington CMDs of young clusters in the Magellanic Clouds (MC) and dSph galaxies in the Local Group (Grebel and collaborators, several papers in preparation/in press).

Such calibrations of the colours do not constitute any kind of proof of formal validity of the method, because of intractable problems with the standard magnitude system and with the passbands. As has been pointed out by other investigators (e.g., Sterken & Manfroid 1992; Manfroid & Sterken 1992; Young 1992a, and references therein), the only fully consistent sets of standards at present are those repeatedly observed with small scatter using a single instrument (telescope + filters + detector) and transformed with identical algorithms. Even though it may be fully consistent for this one instrumental setup, such a system cannot strictly be extended to other types of stars or objects nor can its magnitudes be identified in general with the extra-atmospheric irradiance of the stars unless the atmospheric extinction is removed in accord with the laws of physics. The values of any standard system should be used only with a clear understanding of the usually large systematic errors built into the system.

The physical inverse problem of unambiguously determining the passbands directly from observations of spectrophotometric standards, perhaps modified by model at-

mosphere calculations, seems to us to be almost hopeless because of systematic errors in the scans and the removal atmospheric extinction.

We made only one change to the Bessell passbands. The U passband had to be more sharply attenuated at 320 nm in order both to validate $U-B$ against our calibrating stars and to fit our synthetic $U-B$ isochrones to young MC CMDs. This attenuation is shown in Fig. 1, where we can see a blue shoulder of the U band displaced slightly to the red from the original. Such ad hoc changes to the U passband have been used before (Buser 1978); see the discussion in Sect. 3 of Bell et al. 1994).

U standard magnitudes generally are unphysical because the atmospheric extinction is intentionally not correctly removed – the standard system specifically requires that no color term be used in the extinction removal; in other words, the U standard magnitudes are *not* the U magnitudes outside the atmosphere (Roberts & Grebel 1995a; see also Sterken & Manfroid 1992; Young 1992a). Though the synthetic U magnitudes based on the original U passband are magnitudes outside the atmosphere only the modified U passband provides a synthetic colour that corresponds well to the standard UBV system when Kurucz synthetic spectra and standard (incorrect) photometry transformations for the atmospheric extinction are being used. For consistency we also use the modified passband in the computations of reddening, because the Kurucz spectra are used in every reddening computation. The interstellar reddening in U of the very hottest stars may have to be revisited after U standard magnitudes and the U passband are better understood.

Our Washington CMT_1T_2 passbands were taken from Canterna & Harris (1979). These validate well against observed colours of stars with spectroscopically determined atmospheric parameters, though C is also systematically affected (to a lesser extent) by the incorrect removal of atmospheric extinction. We also have full colour tables, transformations, and isochrones including the DDO51 gravity sensitive supplementary filter to the original Washington system, but we do not present those results in this paper, since they aren't directly relevant to the problem of wideband extinction, which is our focus here.

Theoretical isochrones transformed by us to the Washington system with the same system of passbands and synthetic spectra have been compared by us successfully to CMDs of real stellar populations. We have shown (Roberts & Grebel 1995b) that there is no statistically significant case for a transformation of our synthetic colours to standard; zeropointing is all that is required. We have used our Washington colours successfully in analyzing the metallicity distributions of the stellar populations in the Fornax and Sculptor dSph galaxies (Grebel et al. 1994b,c,d), obtaining – without additional calibration or transformation – metallicity measurements that are in full agreement with the limited spectroscopic data available.

Bell et al. (1994) conclude that magnitude transformations from synthetic to observational always are needed, but in their study of the Washington system (Paltoglou & Bell 1994) they used passbands constructed from modern filters and CCDs, not the standard passbands of Canterna & Harris (1979). Practical experience in photometric reductions with these by the authors has shown that the CCD filter-detector combination for C used by Paltoglou & Bell (1994) has even a significant quadratic colour term in the transformation to the standard passband, so it is not surprising that they require a transformation to the standard system.

We use the interstellar extinction law in the visual range as tabulated by Scheffler (1982) from a variety of sources. Although the dependence of extinction on wavelength is known to vary in the galactic plane, large variations are localised to star forming regions and the Perseus and Cygnus arms, so that an average law will provide valid general results. In Fig. 1 we show the extinction law as fit with cubic splines in the spectral region occupied by the very important metallicity and gravity dependent filters $UBVCM$.

Our synthetic spectra are the well-known grid computed by Kurucz (see, e.g., Buser & Kurucz 1992) comprising 7622 spectra as functions of the three parameters $T_{\rm eff}$ (3500 – 50 000), $\log g$ (0.0–5.0), and [Fe/H] (−5.0 – +1.0). We computed extinction ratios for three luminosity classes, or surface gravities (Table 1): (1) the lowest surface gravity in the grid for that temperature (from luminosity class (LC) I below 8500 K, III at 15 000 K, and V above 40 000 K), (2) 2.5 (LC III), if not the lowest $\log g$, and (3) 5.0 (LC V, above 40 000 K the same as [1]). For simplicity we will refer to the first set of spectra as I or I-II, though there are higher gravities at the hotter temperatures. There are 146 synthetic spectra at solar metallicity. We computed the extinction ratios for the same set of parameters at four metallicities, [Fe/H] = +0.5, 0.0, −1.0, and −2.0, so altogether calculations were done with over 560 synthetic spectra, nine filter passbands, and a single extinction law. In Table 1 we also give our $B-V$, $V-I$, and $M-T_2$ colours for each synthetic spectrum. The spectral energy distributions for the two temperatures below 4000 K may not be reliable, so their colours and the details of their extinction behaviour should be investigated further when better molecular opacities are available.

In Fig. 2 we show the synthetic spectra at several key temperatures at solar metallicity superposed on the blue-visual passbands. These spectra give some insight into the peculiar behaviour of the reddening of the blue colour indices. They are normalised such that the highest flux for each spectrum in the wavelength range is set to 100.0. Figure 2 is a self-contained tour of some obvious causes for the principal features of the extinction curves; we do not duplicate the captions in the text.

Table 1. Temperatures, surface gravities, and temperature colours of the synthetic spectra used in this study. The main sequence set comprises all the highest surface gravities, and the supergiant set the lowest; for the hottest stars these are identical, as shown. The giant set fills in where the $\log g$=2.5 exists and is not the lowest surface gravity. Metallicities of [Fe/H] = +0.5, +0.0, −1.0, −2.0 were studied. This table will also be useful for Paper II

T_{eff}	Supergiant set				Giant set				Main sequence set			
	$\log g$	B–V	V–I	M–T_2	$\log g$	B–V	V–I	M–T_2	$\log g$	B–V	V–I	M–T_2
3500	0.0	1.8480	1.9420	2.4070	2.5	1.3620	1.9390	2.3010	5.0	1.4760	1.8880	2.3220
3750	0.0	1.7750	1.7040	2.1260	2.5	1.4500	1.6590	2.0340	5.0	1.4060	1.6910	2.0890
4000	0.0	1.6340	1.4900	1.8430	2.5	1.3820	1.4770	1.8040	5.0	1.3320	1.5380	1.8950
4250	0.0	1.5010	1.3140	1.6160	2.5	1.2620	1.3050	1.5680	5.0	1.2300	1.3850	1.6890
4500	0.0	1.3660	1.1820	1.4440	2.5	1.1530	1.1540	1.3680	5.0	1.1100	1.2270	1.4690
4750	0.0	1.2290	1.0790	1.3030	2.5	1.0560	1.0330	1.2130	5.0	0.9980	1.0850	1.2720
5000	0.0	1.0900	0.9850	1.1710	2.5	0.9580	0.9390	1.0910	5.0	0.9050	0.9670	1.1130
5250	0.0	0.9530	0.8900	1.0380	2.5	0.8580	0.8580	0.9840	5.0	0.8270	0.8690	0.9860
5500	0.0	0.7980	0.7670	0.8660	2.5	0.7620	0.7840	0.8850	5.0	0.7520	0.7880	0.8840
5750	0.0	0.6660	0.6670	0.7290	2.5	0.6710	0.7120	0.7910	5.0	0.6780	0.7190	0.7950
6000	0.0	0.5380	0.5720	0.5980	2.5	0.5850	0.6420	0.7000	5.0	0.6070	0.6580	0.7160
6250	0.5	0.4370	0.4950	0.4950	2.5	0.5070	0.5730	0.6100	5.0	0.5420	0.6000	0.6440
6500	0.5	0.3330	0.4150	0.3850	2.5	0.4350	0.5060	0.5220	5.0	0.4820	0.5470	0.5770
6750	0.5	0.2500	0.3420	0.2860	2.5	0.3420	0.4000	0.3850	5.0	0.4280	0.4950	0.5120
7000	0.5	0.1830	0.2770	0.2020	2.5	0.2800	0.3330	0.2970	5.0	0.3820	0.4440	0.4490
7250	0.5	0.1380	0.2240	0.1350	2.5	0.2130	0.2690	0.2120	5.0	0.3410	0.3940	0.3870
7500	0.5	0.1350	0.1920	0.1070	2.5	0.1500	0.2100	0.1330	5.0	0.3040	0.3440	0.3260
7750	1.0	0.0610	0.1450	0.0370	2.5	0.1040	0.1590	0.0670	5.0	0.2710	0.2940	0.2650
8000	1.0	0.0560	0.1280	0.0220	2.5	0.0620	0.1160	0.0120	5.0	0.2390	0.2440	0.2040
8250	1.0	0.0630	0.1290	0.0300	2.5	0.0280	0.0800	-0.0340	5.0	0.2020	0.1750	0.1210
8500	1.0	-0.0010	0.0730	-0.0470	2.5	-0.0010	0.0530	-0.0700	5.0	0.1740	0.1290	0.0650
8750	1.5	-0.0060	0.0670	-0.0530	2.5	-0.0230	0.0330	-0.0960	5.0	0.1450	0.0890	0.0140
9000	1.5	-0.0090	0.0630	-0.0560	2.5	-0.0400	0.0160	-0.1170	5.0	0.1110	0.0550	-0.0320
9250	2.0	-0.0450	0.0200	-0.1120	2.5	-0.0510	0.0030	-0.1320	5.0	0.0880	0.0260	-0.0680
9500	2.0	-0.0520	0.0140	-0.1190	2.5	-0.0620	-0.0060	-0.1440	5.0	0.0680	0.0020	-0.0980
9750	2.0	-0.0560	0.0070	-0.1260	2.5	-0.0690	-0.0140	-0.1540	5.0	0.0470	-0.0170	-0.1240
10000	2.0	-0.0610	0.0020	-0.1320	2.5	-0.0760	-0.0220	-0.1620	5.0	0.0300	-0.0350	-0.1460
10500	2.0	-0.0700	-0.0110	-0.1450	2.5	-0.0860	-0.0350	-0.1770	5.0	-0.0030	-0.0620	-0.1820
11000	2.5	-0.0960	-0.0460	-0.1900	2.5	-0.0960	-0.0460	-0.1900	5.0	-0.0300	-0.0810	-0.2090
11500	2.5	-0.1050	-0.0570	-0.2030	2.5	-0.1050	-0.0570	-0.2030	5.0	-0.0510	-0.0960	-0.2290
12000	2.5	-0.1120	-0.0680	-0.2160	2.5	-0.1120	-0.0680	-0.2160	5.0	-0.0670	-0.1080	-0.2450
12500	2.5	-0.1210	-0.0790	-0.2290	2.5	-0.1210	-0.0790	-0.2290	5.0	-0.0810	-0.1180	-0.2600
13000	2.5	-0.1280	-0.0900	-0.2410	2.5	-0.1280	-0.0900	-0.2410	5.0	-0.0920	-0.1270	-0.2720
14000	2.5	-0.1180	-0.0860	-0.2310	2.5	-0.1410	-0.1110	-0.2650	5.0	-0.1110	-0.1440	-0.2930
15000	2.5	-0.1540	-0.1290	-0.2880	2.5	-0.1540	-0.1290	-0.2880	5.0	-0.1270	-0.1580	-0.3120
16000	2.5	-0.1650	-0.1460	-0.3070	2.5	-0.1650	-0.1460	-0.3070	5.0	-0.1420	-0.1710	-0.3300
17000	2.5	-0.1740	-0.1620	-0.3260	2.5	-0.1740	-0.1620	-0.3260	5.0	-0.1550	-0.1850	-0.3470
18000	2.5	-0.1800	-0.1740	-0.3400	2.5	-0.1800	-0.1740	-0.3400	5.0	-0.1680	-0.1970	-0.3620
19000	2.5	-0.1830	-0.1830	-0.3490	2.5	-0.1830	-0.1830	-0.3490	5.0	-0.1790	-0.2090	-0.3780
20000	3.0	-0.2090	-0.2130	-0.3890					5.0	-0.1900	-0.2200	-0.3920
21000	3.0	-0.2140	-0.2220	-0.4000					5.0	-0.1990	-0.2320	-0.4060
22000	3.0	-0.2190	-0.2290	-0.4070					5.0	-0.2090	-0.2410	-0.4190
23000	3.0	-0.2250	-0.2360	-0.4150					5.0	-0.2170	-0.2520	-0.4320
24000	3.0	-0.2310	-0.2440	-0.4250					5.0	-0.2250	-0.2610	-0.4430
25000	3.0	-0.2350	-0.2520	-0.4340					5.0	-0.2310	-0.2710	-0.4550
26000	3.0	-0.2370	-0.2540	-0.4360					5.0	-0.2380	-0.2790	-0.4650
27000	3.5	-0.2560	-0.2820	-0.4710					5.0	-0.2450	-0.2860	-0.4740
28000	3.5	-0.2620	-0.2890	-0.4790					5.0	-0.2510	-0.2940	-0.4830
29000	3.5	-0.2650	-0.2930	-0.4850					5.0	-0.2570	-0.3010	-0.4930
30000	3.5	-0.2670	-0.2940	-0.4860					5.0	-0.2640	-0.3080	-0.5020
31000	3.5	-0.2690	-0.2930	-0.4840					5.0	-0.2700	-0.3150	-0.5100
32000	4.0	-0.2820	-0.3150	-0.5120					5.0	-0.2760	-0.3210	-0.5170
33000	4.0	-0.2840	-0.3160	-0.5130					5.0	-0.2810	-0.3260	-0.5230
34000	4.0	-0.2860	-0.3160	-0.5130					5.0	-0.2860	-0.3300	-0.5290
35000	4.0	-0.2880	-0.3140	-0.5110					5.0	-0.2890	-0.3320	-0.5320
37500	4.5	-0.2970	-0.3270	-0.5270					5.0	-0.2960	-0.3340	-0.5360
40000	4.5	-0.3020	-0.3280	-0.5300					5.0	-0.3010	-0.3350	-0.5360
42500	5.0	-0.3070	-0.3370	-0.5400					5.0	-0.3070	-0.3370	-0.5400
45000	5.0	-0.3110	-0.3400	-0.5440					5.0	-0.3110	-0.3400	-0.5440
47500	5.0	-0.3150	-0.3430	-0.5480					5.0	-0.3150	-0.3430	-0.5480
50000	5.0	-0.3190	-0.3440	-0.5510					5.0	-0.3190	-0.3440	-0.5510

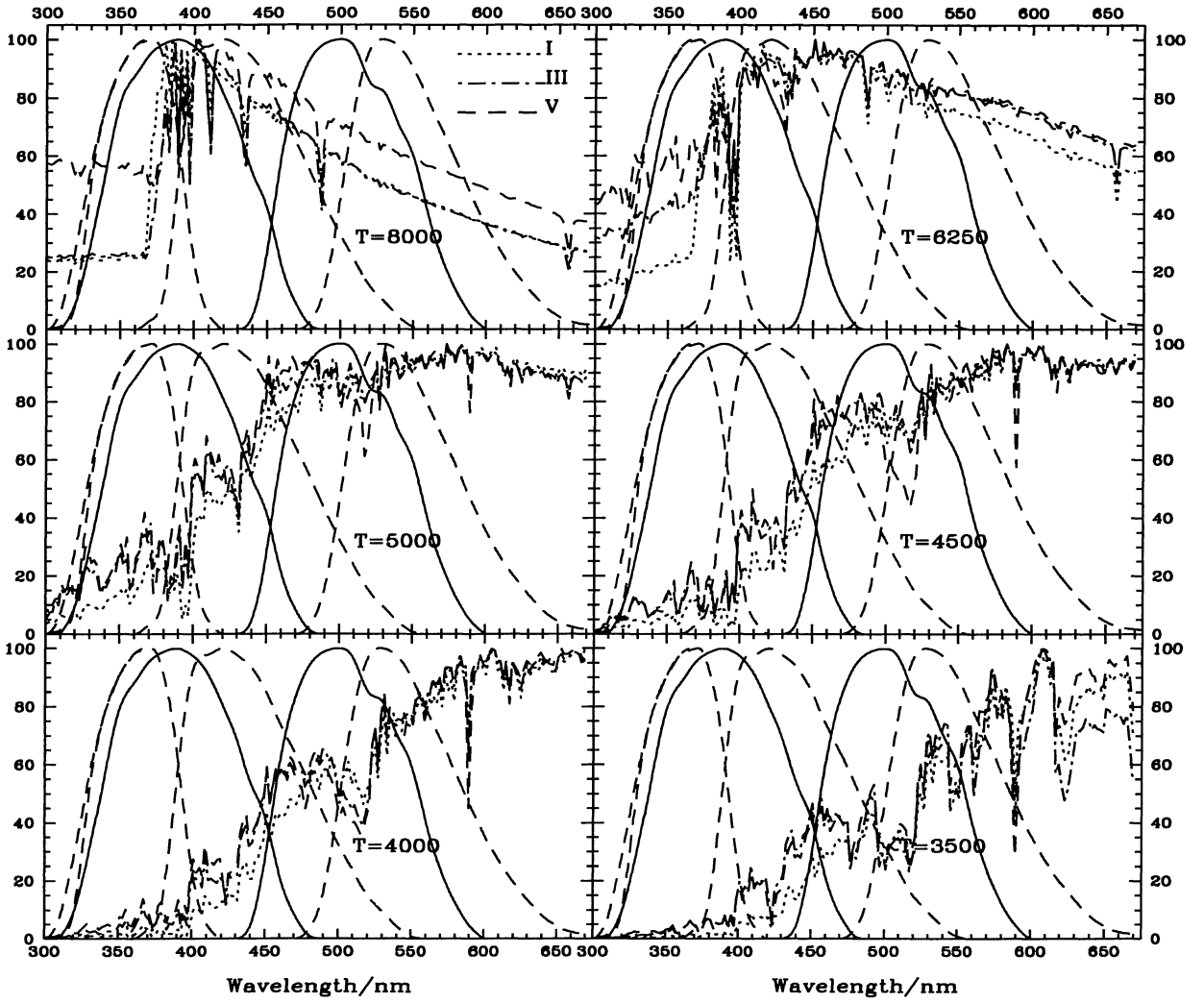

Fig. 2. a)-f) Spectra from Kurucz atmospheres of solar metallicity overlaid on the five "blue" passbands from Fig. 1. a) $T_{\rm eff}$=8000, $B-V$=0.15, $M-T_2$=0.0. Above this temperature the weighting of the U and C passbands shifts progressively from red to blue, as the Balmer jump starts to go away, which increases the relative extinction in the $U-B$ and $C-M$ colour indices, b) $T_{\rm eff}$=6250, $M-T_2$=0.5. At this temperature supergiants (SGs) are reddened much less than MS stars in $C-M$. The spectra show why: the Balmer jump is much greater for the SGs, making the C filter more heavily weighted to the red for these stars. Giants are intermediate, c) $T_{\rm eff}$=5000, $B-V$=1.2 $\simeq M-T_2$. At this temperature all stars suffer almost exactly the same extinctions in $U-B$, $B-V$, and $C-M$, because the spectral energy distributions in the blue vary only weakly with surface gravity. $U-B$ is MORE reddened than for a hot star, because B is weighted to the red, while U is relatively unweighted, for this temperature and all cooler models. $C-M$ is less reddened than for a hot star because C is weighted toward the red, while M is relatively unweighted, d) $T_{\rm eff}$=4500, $B-V$=1.2–1.4, $M-T_2$=1.4. Below $T_{\rm eff}$=5000 the flux in U decreases rapidly, nearly vanishing for supergiants at $T_{\rm eff}$=4000 (K3–4 I). Significant flux remains in the C passband, which is one reason why the Washington filter system is so superior to UBV for cooler stars. The differential reddening in $B-V$ starts to increase toward lower temperatures again for red giants and MS stars as the weighting of B to the red decreases, e) $T_{\rm eff}$=4000, $B-V$=1.3–1.6, $M-T_2$=1.9. The differential reddening of $C-M$ and $B-V$ for SGs is near a minimum here, while that of $U-B$ is near a maximum for the same stars. B, V, C, and M are all weighted the farthest toward the red. It is not obvious what causes the larger reddening in $U-B$, but it isn't relevant, anyway, because these stars are nearly invisible in U, f) $T_{\rm eff}$=3500, $B-V$=1.4–1.9, $M-T_2$=2.3–2.4. These are the coolest of the Kurucz models with types ranging from M3 V to M1–2 I. C has about half the flux in B at this very cool temperature. With the flux decreasing so much in these blue bands, it also gets flatter, so that the differential reddening in all indices tends back toward normal

Each passband was integrated with the spectra at each of 61 temperatures from 3500 K to 50 000 K to provide a flux weighted passband with which to pass through the extinction law. Since the multiplications are commutative, any order would give the same result. The integrations were performed with Simpson's rule at 0.5 nm intervals. The spectra are tabulated at 2 nm intervals in this region. We used Hermite interpolation (Hill 1982) to get to 0.5 nm, because of the jagged texture of the spectra. The much smoother passbands and the extinction law were interpolated to the same interval using cubic splines.

The integrations produce ratios of the passband and colour extinctions to $A_{V,0}$, the V band extinction of a MS star with a temperature of 17 000 K and solar metallicity, typical of B stars (B3–4 V) used for reddening determinations. The Scheffler extinction law, which is tabulated as a ratio A_λ/A_V, must be renormalised for our work, because when multiplied by the V passband and the (17000, 5.0, +0.0) reference spectrum it gives an extinction of 1.01788, instead of 1.000. Thus, $A_{V,0}$ *is defined to be 1.0 throughout this work.*

The renormalised extinction law gives a ratio of total to selective absorption of $R_V=A_V/E_{B-V}=3.346$ at 17 000 K, so we use this value in forming the ratios of the extinctions of the other colours to that of E_{B-V} at 17 000 K. This value for R_V is a little above the range given by Crawford and Mandwewala (1976) of 3.2 ± 0.1. Most workers use 3.0–3.1, while Cardelli et al. (1988, 1989) state that 3.1–3.5 is normal. Krełowski & Papaj (1993) review various methods of measuring and parameterizing interstellar extinction.

Cardelli et al. (1989) and Mathis (1990) define $1/R_V$ as a parameter in an equation giving A_λ/A_V as a function of wavenumber, $< A_\lambda/A_V >= a(x) + B(x)/R_V$, where $x = 1/\lambda$ is the wavenumber, characterizing an average extinction law suitable for extrapolating properties into the UV. But R_V in this equation is not related very closely to the actual reddening ratio of an individual star, as our is. *In this paper, R_V will be understood to be the literal ratio of total to selective extinction for a particular star.* This physical ratio is an important quantity, and is the original meaning of the term R_V. *We show here that R_V, in our definition, is a function not only of the intrinsic properties of the dust, but also of the temperature of the stellar extinction probe and of other properties of the stellar atmosphere.*

We seek to define a *temperature colour*, which is a colour index measuring temperature rather than abundance and which is monotonic with temperature at all surface gravities and abundances. We would like to derive all relations in terms of this observable (after dereddening) temperature colour, in which all the reddening relations are best behaved because it is monotonic with temperature ($U-B$ and $B-V$ are not), and the extinctions as linear as possible.

In the Washington Canterna system that function is well served by the index $M-T_2$, so we will make that colour fundamental to our Washington reddening relations. In the $UBVRI$ system $V-I$ works almost as well, failing only in the same place shared with $M-T_2$ namely $T_{\rm eff}$=3500 K, [Fe/H]=-2.0, $\log g$=5.0, not a very important set of parameters for reddening determinations. Unfortunately, using that index makes finding the $B-V$ reddening from our relations more difficult, and no one uses $V-I$ to define the amount of reddening. Thus we will use $B-V$ as the temperature colour, although it is nonlinear and not as monotonic with temperature. Since Washington reddening laws have not been defined, and only approximate empirical conversions to and from E_{B-V} have been used so far (Geisler et al. 1991), we will define a new internal Washington reddening system in this paper using the temperature colour $M-T_2$ and the T_2 band.

We do not compute reddening free compound colour indices, such as Q, because such general indices for the bluer bands and colours do not in fact exist in our two wide band photometric systems.

Before passing to the results, let us summarise our definitions. Passband is the formal representation of a filter-detector combination, or response function, that one hopes reproduces the standard magnitudes for that system. Nevertheless, the passbands do not define the standard system – the passband is only a formal representation. The standard magnitude system depends both on the defined standard magnitudes and on the reduction methods, right or wrong (Sterken & Manfroid 1992).

Total extinction A_X is the extinction of a passband X. A_V is the extinction of the standard magnitude V and is dependent on the distribution of radiation in the V band, and so on the temperature, surface gravity, and metallicity of the star. $A_{V,0}$ is the total extinction in the V band of the reference stellar spectrum: $T_{\rm eff}$ = 17 000 K, $\log g$=5.0, and [Fe/H] = 0.0.

Differential or selective extinction E is that of a colour like $B-V$ (E_{B-V}), and $E_{(B-V),0}$ is that experienced by a star with the reference spectrum. R_V, the ratio of total to selective extinction for the V band, is A_V/E_{B-V}, $R_{V,0}$ is the ratio for the reference stellar spectrum. The corresponding quantities R_{T2} and $R_{T2,0}$ for the Washington system are defined as $R_{T2}=A_{T2}/E_{M-T2}$, and $R_{T2,0}$ is R_{T2} at the reference spectrum. An extinction law is an extinction curve as a function of wavelength or wavenumber, A_λ/A_V.

3. Results

A summary of the results for $UBVRI$ and WCS is shown in Fig. 3 and Tables 2 and 3. We have plotted the ratios of the differential (selective) extinctions in each important colour index to their reference values. (All MS curves cross at the colour corresponding to $T_{\rm eff}$ = 17 000 K.) In addition we have plotted the same ratios for the

Table 2. Differential (selective) extinctions for the low gravity models at solar metallicity in the colour indices of the $UBVRI$ system

T_{eff}	U–B	E_{U-B}	B–V	E_{B-V}	V–R	E_{V-R}	R–I	E_{R-I}	V–I	E_{V-I}
3500.	2.6840	0.2803	1.8480	0.2568	0.9150	0.1846	1.0270	0.1677	1.9420	0.3523
3750.	2.8420	0.2845	1.7750	0.2516	0.8950	0.1839	0.8090	0.1672	1.7040	0.3512
4000.	2.6600	0.2895	1.6340	0.2489	0.8010	0.1866	0.6890	0.1687	1.4900	0.3553
4250.	2.2600	0.2951	1.5010	0.2502	0.7110	0.1878	0.6030	0.1710	1.3140	0.3588
4500.	1.8200	0.2949	1.3660	0.2542	0.6410	0.1884	0.5410	0.1727	1.1820	0.3611
4750.	1.4450	0.2898	1.2290	0.2590	0.5850	0.1893	0.4940	0.1739	1.0790	0.3632
5000.	1.1510	0.2820	1.0900	0.2637	0.5280	0.1904	0.4570	0.1750	0.9850	0.3654
5250.	0.9160	0.2732	0.9530	0.2682	0.4720	0.1913	0.4180	0.1764	0.8900	0.3677
5500.	0.7880	0.2609	0.7980	0.2723	0.3990	0.1920	0.3680	0.1786	0.7670	0.3706
5750.	0.6520	0.2507	0.6660	0.2766	0.3420	0.1924	0.3250	0.1804	0.6670	0.3728
6000.	0.5480	0.2408	0.5380	0.2807	0.2870	0.1927	0.2850	0.1823	0.5720	0.3750
6250.	0.4460	0.2348	0.4370	0.2845	0.2450	0.1930	0.2500	0.1834	0.4950	0.3763
6500.	0.3900	0.2266	0.3330	0.2876	0.1990	0.1932	0.2160	0.1850	0.4150	0.3782
6750.	0.3340	0.2202	0.2500	0.2901	0.1580	0.1933	0.1840	0.1866	0.3420	0.3799
7000.	0.2730	0.2154	0.1830	0.2922	0.1220	0.1934	0.1550	0.1879	0.2770	0.3813
7250.	0.2090	0.2128	0.1380	0.2937	0.0930	0.1933	0.1310	0.1890	0.2240	0.3823
7500.	0.1300	0.2141	0.1350	0.2944	0.0810	0.1930	0.1110	0.1894	0.1920	0.3824
7750.	0.1240	0.2103	0.0610	0.2962	0.0560	0.1933	0.0890	0.1899	0.1450	0.3832
8000.	0.0460	0.2122	0.0560	0.2968	0.0490	0.1932	0.0790	0.1900	0.1280	0.3832
8250.	-0.0420	0.2160	0.0630	0.2974	0.0550	0.1931	0.0740	0.1894	0.1290	0.3825
8500.	-0.0130	0.2123	-0.0010	0.2981	0.0230	0.1933	0.0500	0.1903	0.0730	0.3837
8750.	-0.0760	0.2147	-0.0060	0.2986	0.0230	0.1933	0.0440	0.1902	0.0670	0.3835
9000.	-0.1370	0.2175	-0.0090	0.2989	0.0230	0.1933	0.0400	0.1899	0.0630	0.3832
9250.	-0.1060	0.2158	-0.0450	0.2991	0.0000	0.1933	0.0200	0.1904	0.0200	0.3837
9500.	-0.1550	0.2178	-0.0520	0.2994	-0.0010	0.1933	0.0150	0.1904	0.0140	0.3836
9750.	-0.2010	0.2199	-0.0560	0.2996	-0.0030	0.1932	0.0100	0.1903	0.0070	0.3835
10000.	-0.2450	0.2219	-0.0610	0.2998	-0.0040	0.1932	0.0060	0.1902	0.0020	0.3834
10500.	-0.3250	0.2257	-0.0700	0.3001	-0.0080	0.1932	-0.0030	0.1900	-0.0110	0.3832
11000.	-0.3240	0.2261	-0.0960	0.3001	-0.0240	0.1932	-0.0220	0.1903	-0.0460	0.3834
11500.	-0.3850	0.2287	-0.1050	0.3003	-0.0280	0.1932	-0.0290	0.1902	-0.0570	0.3834
12000.	-0.4390	0.2308	-0.1120	0.3005	-0.0330	0.1931	-0.0350	0.1902	-0.0680	0.3834
12500.	-0.4860	0.2325	-0.1210	0.3007	-0.0370	0.1931	-0.0420	0.1902	-0.0790	0.3834
13000.	-0.5270	0.2340	-0.1280	0.3008	-0.0420	0.1931	-0.0480	0.1903	-0.0900	0.3834
14000.	-0.6810	0.2401	-0.1180	0.3010	-0.0370	0.1931	-0.0490	0.1899	-0.0860	0.3830
15000.	-0.6640	0.2386	-0.1540	0.3013	-0.0590	0.1931	-0.0700	0.1905	-0.1290	0.3835
16000.	-0.7240	0.2404	-0.1650	0.3015	-0.0660	0.1931	-0.0800	0.1906	-0.1460	0.3836
17000.	-0.7790	0.2421	-0.1740	0.3016	-0.0720	0.1930	-0.0900	0.1907	-0.1620	0.3837
18000.	-0.8320	0.2438	-0.1800	0.3017	-0.0770	0.1930	-0.0970	0.1907	-0.1740	0.3837
19000.	-0.8860	0.2454	-0.1830	0.3019	-0.0810	0.1930	-0.1020	0.1907	-0.1830	0.3837
20000.	-0.8510	0.2438	-0.2090	0.3019	-0.0960	0.1930	-0.1170	0.1911	-0.2130	0.3841
21000.	-0.8900	0.2449	-0.2140	0.3020	-0.0990	0.1929	-0.1230	0.1912	-0.2220	0.3841
22000.	-0.9270	0.2458	-0.2190	0.3022	-0.1020	0.1929	-0.1270	0.1912	-0.2290	0.3841
23000.	-0.9580	0.2465	-0.2250	0.3024	-0.1060	0.1929	-0.1300	0.1913	-0.2360	0.3842
24000.	-0.9860	0.2470	-0.2310	0.3025	-0.1090	0.1929	-0.1350	0.1914	-0.2440	0.3843
25000.	-1.0130	0.2476	-0.2350	0.3027	-0.1130	0.1929	-0.1390	0.1914	-0.2520	0.3843
26000.	-1.0410	0.2483	-0.2370	0.3028	-0.1120	0.1928	-0.1420	0.1914	-0.2540	0.3842
27000.	-1.0050	0.2470	-0.2560	0.3027	-0.1270	0.1928	-0.1550	0.1918	-0.2820	0.3846
28000.	-1.0250	0.2474	-0.2620	0.3028	-0.1300	0.1928	-0.1590	0.1919	-0.2890	0.3847
29000.	-1.0460	0.2477	-0.2650	0.3030	-0.1320	0.1927	-0.1610	0.1919	-0.2930	0.3847
30000.	-1.0650	0.2481	-0.2670	0.3031	-0.1310	0.1927	-0.1630	0.1919	-0.2940	0.3846
31000.	-1.0810	0.2484	-0.2690	0.3033	-0.1300	0.1927	-0.1630	0.1919	-0.2930	0.3846
32000.	-1.0630	0.2480	-0.2820	0.3031	-0.1410	0.1927	-0.1740	0.1922	-0.3150	0.3849
33000.	-1.0770	0.2481	-0.2840	0.3032	-0.1410	0.1927	-0.1750	0.1921	-0.3160	0.3848
34000.	-1.0890	0.2482	-0.2860	0.3034	-0.1410	0.1927	-0.1750	0.1921	-0.3160	0.3848
35000.	-1.0980	0.2483	-0.2880	0.3035	-0.1390	0.1927	-0.1750	0.1921	-0.3140	0.3848
37500.	-1.1050	0.2484	-0.2970	0.3035	-0.1460	0.1927	-0.1810	0.1922	-0.3270	0.3849
40000.	-1.1180	0.2484	-0.3020	0.3037	-0.1450	0.1927	-0.1830	0.1922	-0.3280	0.3849
42500.	-1.1250	0.2486	-0.3070	0.3036	-0.1500	0.1927	-0.1870	0.1923	-0.3370	0.3850
45000.	-1.1330	0.2486	-0.3110	0.3038	-0.1510	0.1927	-0.1890	0.1923	-0.3400	0.3850
47500.	-1.1400	0.2485	-0.3150	0.3039	-0.1520	0.1927	-0.1910	0.1923	-0.3430	0.3850
50000.	-1.1460	0.2485	-0.3190	0.3040	-0.1520	0.1927	-0.1920	0.1924	-0.3440	0.3851

principal magnitude V of the $UBVRI$ system, and our choice for the principal magnitude in the WCS system, T_2. For the reference spectrum with the adopted extinction law we have $R_{V,0}$=3.34775 and $R_{T2,0}$=1.25513. We have plotted these normalised curves for $UBVRI$ vs. $V-I$ because we are showing the qualitative behaviour of the extinction in the different colours, which is best shown with the very temperature sensitive colour $V-I$, and because $V-I$ is the most like the Washington colour $M-T_2$, so that overall comparisons between the systems are facilitated.

The actual relative extinctions for the main sequence at solar metallicity for both $UBVRI$ and Washington systems is presented in the two part Table 4.

Table 3. Differential (selective) extinctions for the low gravity models at solar metallicity in the colour indices of the Washington system

T_{eff}	C–M	E_{C-M}	M–T_1	E_{M-T1}	T_1–T_2	E_{T1-T2}	M–T_2	E_{M-T2}
3500.	2.2730	0.2460	1.3480	0.2575	1.0590	0.1993	2.4070	0.4568
3750.	2.3280	0.2376	1.3030	0.2651	0.8230	0.1951	2.1260	0.4602
4000.	2.1990	0.2381	1.1530	0.2702	0.6900	0.1941	1.8430	0.4643
4250.	2.0000	0.2451	1.0210	0.2729	0.5950	0.1944	1.6160	0.4673
4500.	1.7670	0.2546	0.9190	0.2752	0.5250	0.1947	1.4440	0.4699
4750.	1.5330	0.2633	0.8260	0.2777	0.4770	0.1949	1.3030	0.4726
5000.	1.3110	0.2699	0.7340	0.2802	0.4370	0.1952	1.1710	0.4754
5250.	1.1080	0.2748	0.6430	0.2824	0.3950	0.1956	1.0380	0.4781
5500.	0.9220	0.2747	0.5260	0.2851	0.3400	0.1964	0.8660	0.4815
5750.	0.7520	0.2763	0.4360	0.2870	0.2930	0.1970	0.7290	0.4840
6000.	0.5980	0.2770	0.3490	0.2889	0.2490	0.1977	0.5980	0.4865
6250.	0.4710	0.2789	0.2840	0.2902	0.2110	0.1979	0.4950	0.4881
6500.	0.3570	0.2786	0.2120	0.2917	0.1730	0.1985	0.3850	0.4901
6750.	0.2650	0.2789	0.1480	0.2927	0.1380	0.1990	0.2860	0.4917
7000.	0.1840	0.2799	0.0970	0.2934	0.1050	0.1995	0.2020	0.4930
7250.	0.1230	0.2818	0.0580	0.2938	0.0770	0.1999	0.1350	0.4937
7500.	0.0870	0.2859	0.0500	0.2933	0.0570	0.2001	0.1070	0.4933
7750.	0.0260	0.2840	0.0030	0.2945	0.0340	0.2000	0.0370	0.4945
8000.	-0.0110	0.2878	-0.0010	0.2943	0.0230	0.2000	0.0220	0.4943
8250.	-0.0440	0.2927	0.0110	0.2940	0.0190	0.1996	0.0300	0.4937
8500.	-0.0780	0.2892	-0.0410	0.2951	-0.0060	0.1998	-0.0470	0.4950
8750.	-0.1080	0.2923	-0.0420	0.2951	-0.0110	0.1997	-0.0530	0.4948
9000.	-0.1360	0.2954	-0.0420	0.2951	-0.0140	0.1996	-0.0560	0.4947
9250.	-0.1490	0.2928	-0.0760	0.2957	-0.0360	0.1995	-0.1120	0.4953
9500.	-0.1730	0.2951	-0.0780	0.2958	-0.0410	0.1995	-0.1190	0.4953
9750.	-0.1950	0.2974	-0.0810	0.2958	-0.0450	0.1994	-0.1260	0.4952
10000.	-0.2180	0.2996	-0.0830	0.2959	-0.0490	0.1993	-0.1320	0.4952
10500.	-0.2580	0.3037	-0.0880	0.2960	-0.0570	0.1991	-0.1450	0.4951
11000.	-0.2740	0.3030	-0.1140	0.2964	-0.0760	0.1990	-0.1900	0.4955
11500.	-0.3070	0.3062	-0.1200	0.2965	-0.0830	0.1990	-0.2030	0.4955
12000.	-0.3370	0.3089	-0.1270	0.2966	-0.0890	0.1989	-0.2160	0.4955
12500.	-0.3640	0.3113	-0.1330	0.2967	-0.0960	0.1989	-0.2290	0.4956
13000.	-0.3890	0.3134	-0.1400	0.2968	-0.1010	0.1988	-0.2410	0.4957
14000.	-0.4580	0.3225	-0.1300	0.2966	-0.1010	0.1987	-0.2310	0.4953
15000.	-0.4740	0.3205	-0.1640	0.2972	-0.1240	0.1988	-0.2880	0.4959
16000.	-0.5120	0.3235	-0.1740	0.2973	-0.1330	0.1987	-0.3070	0.4960
17000.	-0.5460	0.3265	-0.1840	0.2974	-0.1420	0.1987	-0.3260	0.4961
18000.	-0.5780	0.3294	-0.1900	0.2974	-0.1500	0.1987	-0.3400	0.4961
19000.	-0.6100	0.3324	-0.1940	0.2975	-0.1550	0.1986	-0.3490	0.4961
20000.	-0.6070	0.3297	-0.2190	0.2979	-0.1700	0.1987	-0.3890	0.4966
21000.	-0.6330	0.3319	-0.2240	0.2979	-0.1760	0.1987	-0.4000	0.4966
22000.	-0.6570	0.3339	-0.2280	0.2980	-0.1790	0.1987	-0.4070	0.4967
23000.	-0.6790	0.3355	-0.2320	0.2980	-0.1830	0.1987	-0.4150	0.4967
24000.	-0.7000	0.3370	-0.2370	0.2981	-0.1880	0.1987	-0.4250	0.4968
25000.	-0.7180	0.3384	-0.2410	0.2981	-0.1930	0.1987	-0.4340	0.4968
26000.	-0.7370	0.3400	-0.2410	0.2981	-0.1950	0.1987	-0.4360	0.4968
27000.	-0.7270	0.3374	-0.2640	0.2984	-0.2070	0.1988	-0.4710	0.4972
28000.	-0.7440	0.3384	-0.2670	0.2985	-0.2120	0.1988	-0.4790	0.4973
29000.	-0.7590	0.3395	-0.2700	0.2985	-0.2150	0.1988	-0.4850	0.4973
30000.	-0.7720	0.3405	-0.2690	0.2985	-0.2170	0.1988	-0.4860	0.4973
31000.	-0.7830	0.3414	-0.2680	0.2985	-0.2160	0.1988	-0.4840	0.4973
32000.	-0.7810	0.3401	-0.2850	0.2987	-0.2270	0.1988	-0.5120	0.4975
33000.	-0.7910	0.3408	-0.2850	0.2987	-0.2280	0.1988	-0.5130	0.4975
34000.	-0.8000	0.3414	-0.2840	0.2987	-0.2290	0.1988	-0.5130	0.4975
35000.	-0.8070	0.3419	-0.2830	0.2988	-0.2280	0.1988	-0.5110	0.4976
37500.	-0.8180	0.3421	-0.2920	0.2989	-0.2350	0.1988	-0.5270	0.4977
40000.	-0.8290	0.3426	-0.2930	0.2990	-0.2370	0.1988	-0.5300	0.4978
42500.	-0.8370	0.3429	-0.2990	0.2991	-0.2410	0.1988	-0.5400	0.4978
45000.	-0.8460	0.3432	-0.3010	0.2992	-0.2430	0.1987	-0.5440	0.4979
47500.	-0.8520	0.3434	-0.3040	0.2992	-0.2440	0.1987	-0.5480	0.4980
50000.	-0.8580	0.3436	-0.3050	0.2993	-0.2460	0.1988	-0.5510	0.4981

Though our Wildey extinctions were computed spectrum by spectrum, each at a specific $T_{\rm eff}$, we instead plot the extinction ratios versus the measurable temperature colour for each system, which is of course one of our synthetic colours computed from the same Kurucz synthetic spectra, using the same passbands, and zeropointed using a robust Lorentzian least squares fit (see Press et al. 1992, p. 696: NR). Although the intrinsic temperature colour may not be directly observable with the same accuracy as spectral type, it is much easier to measure than spectral type, is related to the spectral energy distribution, and is more observable than $T_{\rm eff}$. Since our reddening computations assume the moderate extinction $A_{V,0} = 1.0$, the observed colour will do well enough for computing the value

Table 4. Total extinction A_X relative to $A_{X0} = 1.0$ at $T_{\rm eff} = 17\,000$ K for the low gravity models at solar metallicity in the bands $UBVRI$ and CMT_1T_2. There are two bands defined for B, with BX including the deformation of atmospheric extinction, and used only with $U[X]$, whose blue cutoff is *defined* by atmospheric extinction (after Bessell)

$T_{\rm eff}$	A_{UX}	A_{BX}	A_B	A_V	A_R	A_I	R_V	A_C	A_M	A_{T1}	A_{T2}	R_{T2}
3500.	1.48944	1.20917	1.21119	0.95441	0.76978	0.60209	3.71683	1.31496	1.06900	0.81154	0.61225	1.34044
3750.	1.49120	1.20671	1.20853	0.95693	0.77298	0.60577	3.80332	1.31207	1.07443	0.80935	0.61424	1.33472
4000.	1.49922	1.20974	1.21169	0.96274	0.77619	0.60746	3.86726	1.31786	1.07977	0.80956	0.61545	1.32547
4250.	1.51036	1.21524	1.21743	0.96725	0.77948	0.60847	3.86617	1.32860	1.08354	0.81060	0.61624	1.31871
4500.	1.51704	1.22214	1.22461	0.97040	0.78198	0.60928	3.81733	1.34126	1.08669	0.81145	0.61680	1.31265
4750.	1.51915	1.22940	1.23212	0.97312	0.78380	0.60992	3.75711	1.35307	1.08977	0.81208	0.61717	1.30589
5000.	1.51860	1.23658	1.23953	0.97584	0.78542	0.61040	3.70083	1.36276	1.09287	0.81268	0.61743	1.29866
5250.	1.51671	1.24353	1.24668	0.97847	0.78717	0.61079	3.64809	1.37058	1.09576	0.81333	0.61768	1.29201
5500.	1.51148	1.25057	1.25387	0.98158	0.78961	0.61101	3.60500	1.37404	1.09936	0.81429	0.61788	1.28331
5750.	1.50781	1.25710	1.26056	0.98397	0.79161	0.61116	3.55750	1.37832	1.10207	0.81505	0.61804	1.27686
6000.	1.50414	1.26334	1.26695	0.98622	0.79351	0.61120	3.51316	1.38166	1.10464	0.81579	0.61812	1.27051
6250.	1.50344	1.26864	1.27238	0.98792	0.79497	0.61158	3.47295	1.38545	1.10654	0.81635	0.61847	1.26717
6500.	1.50017	1.27357	1.27740	0.98979	0.79658	0.61155	3.44133	1.38721	1.10863	0.81698	0.61851	1.26197
6750.	1.49780	1.27757	1.28149	0.99140	0.79807	0.61151	3.41757	1.38915	1.11026	0.81756	0.61854	1.25790
7000.	1.49630	1.28093	1.28493	0.99276	0.79939	0.61146	3.39800	1.39142	1.11151	0.81808	0.61854	1.25470
7250.	1.49614	1.28337	1.28744	0.99379	0.80048	0.61150	3.38424	1.39406	1.11227	0.81850	0.61858	1.25298
7500.	1.49848	1.28434	1.28850	0.99411	0.80114	0.61169	3.37677	1.39790	1.11203	0.81874	0.61868	1.25406
7750.	1.49755	1.28725	1.29140	0.99525	0.80191	0.61206	3.36062	1.39763	1.11358	0.81903	0.61908	1.25191
8000.	1.50021	1.28805	1.29226	0.99543	0.80224	0.61223	3.35360	1.40129	1.11347	0.81915	0.61915	1.25252
8250.	1.50442	1.28839	1.29264	0.99520	0.80210	0.61268	3.34589	1.40576	1.11306	0.81906	0.61941	1.25475
8500.	1.50273	1.29040	1.29461	0.99646	0.80313	0.61281	3.34218	1.40381	1.11460	0.81947	0.61964	1.25192
8750.	1.50552	1.29084	1.29508	0.99649	0.80321	0.61302	3.33736	1.40689	1.11459	0.81949	0.61975	1.25245
9000.	1.50864	1.29117	1.29542	0.99648	0.80322	0.61331	3.33339	1.41000	1.11458	0.81947	0.61992	1.25323
9250.	1.50798	1.29218	1.29638	0.99731	0.80398	0.61356	3.33463	1.40830	1.11550	0.81978	0.62023	1.25230
9500.	1.51031	1.29251	1.29672	0.99737	0.80408	0.61373	3.33170	1.41072	1.11558	0.81980	0.62033	1.25254
9750.	1.51265	1.29278	1.29701	0.99742	0.80417	0.61392	3.32938	1.41308	1.11567	0.81983	0.62044	1.25286
10000.	1.51492	1.29302	1.29725	0.99748	0.80426	0.61410	3.32745	1.41536	1.11574	0.81985	0.62056	1.25320
10500.	1.51909	1.29344	1.29769	0.99761	0.80442	0.61444	3.32454	1.41964	1.11591	0.81990	0.62078	1.25378
11000.	1.52019	1.29408	1.29829	0.99823	0.80505	0.61479	3.32671	1.41960	1.11656	0.82014	0.62111	1.25362
11500.	1.52312	1.29446	1.29868	0.99838	0.80523	0.61500	3.32457	1.42289	1.11673	0.82020	0.62124	1.25380
12000.	1.52559	1.29481	1.29904	0.99854	0.80540	0.61519	3.32297	1.42579	1.11690	0.82026	0.62136	1.25391
12500.	1.52768	1.29514	1.29937	0.99871	0.80558	0.61535	3.32171	1.42834	1.11706	0.82032	0.62146	1.25396
13000.	1.52949	1.29545	1.29969	0.99888	0.80575	0.61549	3.32068	1.43063	1.11722	0.82038	0.62155	1.25398
14000.	1.53556	1.29548	1.29978	0.99873	0.80560	0.61573	3.31757	1.43937	1.11690	0.82030	0.62164	1.25516
15000.	1.53509	1.29652	1.30078	0.99950	0.80641	0.61596	3.31758	1.43824	1.11778	0.82062	0.62186	1.25397
16000.	1.53733	1.29696	1.30123	0.99977	0.80671	0.61614	3.31646	1.44153	1.11801	0.82072	0.62199	1.25395
17000.	1.53940	1.29732	1.30160	1.00000	0.80697	0.61631	3.31563	1.44467	1.11820	0.82082	0.62210	1.25398
18000.	1.54137	1.29761	1.30191	1.00018	0.80719	0.61647	3.31480	1.44775	1.11832	0.82089	0.62220	1.25412
19000.	1.54327	1.29784	1.30215	1.00028	0.80732	0.61660	3.31369	1.45080	1.11838	0.82092	0.62228	1.25434
20000.	1.54231	1.29847	1.30274	1.00084	0.80789	0.61676	3.31509	1.44874	1.11903	0.82116	0.62244	1.25342
21000.	1.54362	1.29873	1.30302	1.00097	0.80804	0.61686	3.31398	1.45100	1.11913	0.82120	0.62250	1.25345
22000.	1.54477	1.29899	1.30329	1.00109	0.80815	0.61694	3.31267	1.45307	1.11922	0.82124	0.62254	1.25343
23000.	1.54573	1.29927	1.30357	1.00121	0.80827	0.61701	3.31127	1.45484	1.11931	0.82128	0.62258	1.25335
24000.	1.54656	1.29954	1.30385	1.00133	0.80842	0.61707	3.31003	1.45639	1.11942	0.82133	0.62262	1.25326
25000.	1.54738	1.29976	1.30408	1.00143	0.80857	0.61714	3.30886	1.45789	1.11949	0.82139	0.62266	1.25327
26000.	1.54823	1.29990	1.30422	1.00143	0.80863	0.61718	3.30742	1.45946	1.11948	0.82141	0.62269	1.25340
27000.	1.54736	1.30033	1.30462	1.00194	0.80911	0.61733	3.31025	1.45739	1.12003	0.82160	0.62281	1.25261
28000.	1.54793	1.30057	1.30487	1.00204	0.80926	0.61738	3.30896	1.45855	1.12011	0.82166	0.62285	1.25258
29000.	1.54848	1.30076	1.30506	1.00209	0.80934	0.61742	3.30749	1.45966	1.12015	0.82168	0.62288	1.25258
30000.	1.54896	1.30090	1.30521	1.00208	0.80936	0.61745	3.30587	1.46068	1.12016	0.82169	0.62289	1.25263
31000.	1.54935	1.30100	1.30531	1.00205	0.80933	0.61746	3.30423	1.46153	1.12016	0.82167	0.62290	1.25266
32000.	1.54921	1.30124	1.30552	1.00244	0.80974	0.61759	3.30754	1.46065	1.12052	0.82184	0.62300	1.25218
33000.	1.54950	1.30138	1.30567	1.00245	0.80976	0.61761	3.30597	1.46137	1.12054	0.82184	0.62301	1.25221
34000.	1.54973	1.30151	1.30580	1.00244	0.80974	0.61762	3.30440	1.46197	1.12056	0.82183	0.62302	1.25223
35000.	1.54991	1.30161	1.30591	1.00242	0.80970	0.61762	3.30295	1.46245	1.12058	0.82181	0.62303	1.25218
37500.	1.55028	1.30183	1.30611	1.00263	0.80992	0.61771	3.30375	1.46286	1.12080	0.82190	0.62310	1.25198
40000.	1.55048	1.30207	1.30636	1.00266	0.80993	0.61772	3.30141	1.46350	1.12090	0.82190	0.62313	1.25183
42500.	1.55079	1.30216	1.30644	1.00279	0.81008	0.61780	3.30245	1.46390	1.12104	0.82196	0.62319	1.25180
45000.	1.55091	1.30235	1.30663	1.00284	0.81012	0.61782	3.30108	1.46430	1.12113	0.82197	0.62322	1.25167
47500.	1.55101	1.30250	1.30679	1.00288	0.81017	0.61784	3.30002	1.46463	1.12122	0.82198	0.62323	1.25152
50000.	1.55109	1.30263	1.30691	1.00292	0.81021	0.61784	3.29916	1.46492	1.12129	0.82199	0.62324	1.25135

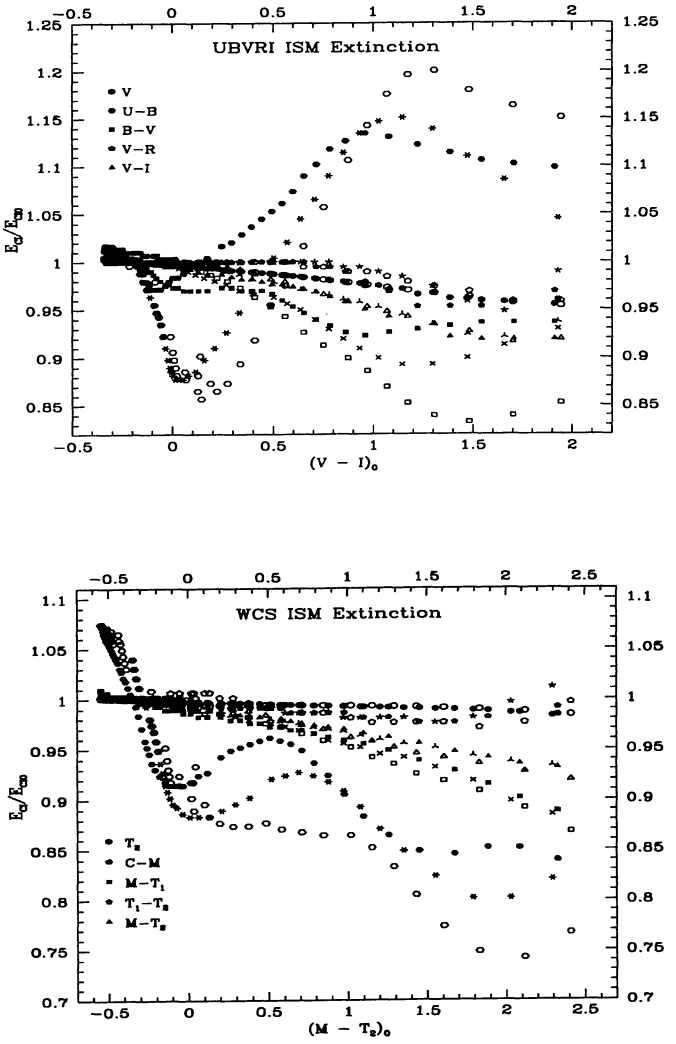

Fig. 3. a) and b) Differential extinctions relative to those suffered by the reference spectrum discussed in the text. Filled polygons are main sequence ($\log g$=5.0), skeleton (star) figures are giants of intermediate surface gravity (2.5), and hollow polygons are the most luminous stars of that temperature. This code will be used in subsequent figures. Note that in both plots the temperature colour can be seen represented by triangles. The gap near CI=0.2 in both plots is caused by the sudden onset of the Balmer jump, when the stellar flux is redistributed. The irregularity in the supergiant curves is caused by sudden jumps in the lowest surface gravity in the grid adopted by Buser & Kurucz (1992). See Table 1. a) $UBVRI$ extinction. Only V and the $V-I$ have extinctions whose variations can accurately be represented by straight lines, and which do not depend on luminosity class. b) WCS extinction. Other than $C-M$, the other indices are better behaved than those of $UBVRI$. $M-T_2$ shows only half as much drop in reddening as does $B-V$, but its differential reddening is larger, because the spectral baseline is longer

of the colour temperature to insert into a formula for the colour dependent extinction after one iteration. We will return to such practical matters in Sect. 5.

The most striking feature of Fig. 3 is the dramatically different colour-dependent behaviour of $U-B$ and $C-M$ from that of the other colours and from each other. To our knowledge, this behaviour has not been shown before. The second most striking feature is the strong differences of the colour dependence of extinction of the evolved stars from that of the MS stars in $U-B$, $C-M$, and for the cool stars in $B-V$. Before we discuss numerical approximation methods that can be used to incorporate our results in dereddening programs, we mention a few possible astrophysical implications of the reddening behaviour we have discovered.

Though we have computed the complete set of results for three surface gravities and four metallicities, we present here the plots and fits for the colour dependences of extinction for the three luminosity classes only with solar metallicity, and for the three non-solar metallicities only for the giants, that is, the intermediate surface gravity models. In Fig. 4 we show the dependence of the extinctions of U and $U-B$ on $B-V$ among different luminosity classes for solar metallicity, and among different metallicities for giants.

The sharp dip in relative extinction of $U-B$ of main sequence stars near $B-V \simeq 0.0$ creates problems for fitting $U-B$ isochrones to reddened young clusters. ($U-B$ isochrones give greater age discrimination in young clusters than do $B-V$). The rapid drop in relative extinction, if not properly corrected, would make the upper MS appear too steep and could cause a younger age to be assigned and more reddening than is the case. The same effect, though weaker, also applies to CMDs in $B-V$. Similarly, dereddening the evolved stars the same amount as the MS stars could lead to a substantial overestimate of their luminosity, also biasing the judgement of the observer toward incorrectly young ages for reddened young and intermediate aged clusters. Dereddening of stars correctly throughout a CMD is challenging, and we have not supplied a complete solution here. Being able to do so would be very advantageous in correctly dereddening a cluster of age $t \sim 10^8$ yr, for instance.

The only Washington colour showing variations of extinction with temperature, $C-M$, presents a different set of problems from that of $U-B$ or $B-V$. The extinction drops very rapidly with temperature for the hotter stars of all luminosity classes, reaching a minimum near A0, which distorts the apparent colour of the main sequences of reddened clusters having turnoffs at A0 and blueward, making them more vertical in $C-M$. However, with $C-M$ one can apply the same linear extinction colour dependence to all stars blueward of $M-T_2$=0.0.

In C and $C-M$, evolving stars cooler than A0 part company with the main sequence in their reddening be-

haviour. Below 5500 K the evolved stars continue to suffer less and less extinction in C and $C-M$. This behaviour, combined with C's coverage of half of the B band, helps $C-M$ retain its usefulness to far redder and more reddened stars than does $U-B$: K supergiants suffer 15% less extinction in C than they do in U, and they have vastly more flux in C than in U, as can be seen in Fig. 2. Thus, *reddened older populations can be dereddened more easily in Washington than in UBVRI*, as well as analyzed more completely and accurately.

Few of these relations expressing the dependence of interstellar extinction on temperature colour can be fit usefully with power series of practical order, say, quartic. Polynomials of higher order tend to have ripples not found in the data. We found the extinction curves to be fit quite easily with ratios of polynomials of moderate order (≤ 6)

$$P_{mk}(x) = (p_0+p_1x+...+p_mx^m)/(1+q_1x+...+q_kx^k) \quad (1)$$

Fortunately, an excellent subroutine for such fits is readily available with an adequate explanation of the algorithm, which uses minimax methods with Chebyshev polynomials (Press et al. 1992, pp. 197-201).

We have experimented to find the combination of upper and lower powers with the lowest order that would provide a curve making a good qualitative and quantitative fit reproducing the behaviour of the extinction data, and that would not exhibit singularities (one failure of the NR routine). However, it was not possible to search systematically for the simplest ratio in every case, so there are doubtless some simpler solutions that are at least equally good. Taste or need might determine whether or not to accept fits with lower powers and greater deviations. Tables of all fits shown in this paper and other similar fits for other sets of stellar parameters will be available electronically from the Simbad database.

Returning to Fig. 4, we note again the very strong nonlinear dependence of the reddening in U and $U-B$ on both the colour of the star and its surface gravity. However, thanks to a signal limitation of the U filter – cool stars are for all practical purposes invisible in it – the part of the behaviour in the right side of the plot is not of practical significance. Another mitigating factor is that, for the hotter stars we are mainly concerned about dereddening the upper main sequence and the blue supergiants and for that we can use the steep straight line. Because of the steepness of the line, accurate photometry is vital. Dereddening the F supergiants and LBVs requires more care, and the exact rational polynomial should be used.

The Washington violet filter C and the $C-M$ colour index also are shown in Fig 4. The upper part of the reddening curves is as steep as those of U and $U-B$, also requiring good photometry to implement correct dereddening. The remainder of the curves behave much more independently of surface gravity than do those of U and $U-B$.

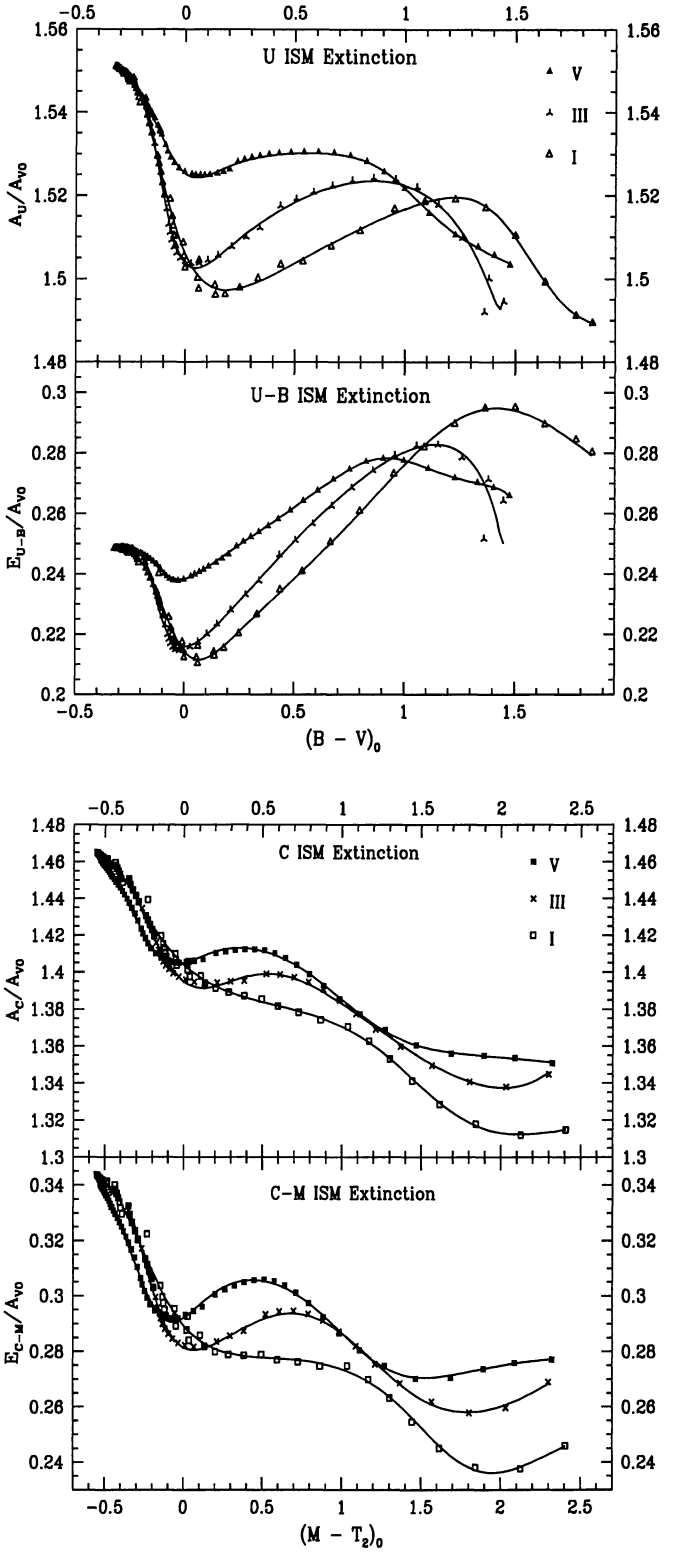

Fig. 4. a) and b) Comparison plots of selective and total extinctions of the most troublesome colour and band in each of the two filter systems. We plot all three surface gravities at solar metallicity with our usual convention: solid is MS, skeletal is giants, hollow is SG. Overplotted are the rational polynomials fitted to each gravity. a) U, $U-B$, b) C, $C-M$

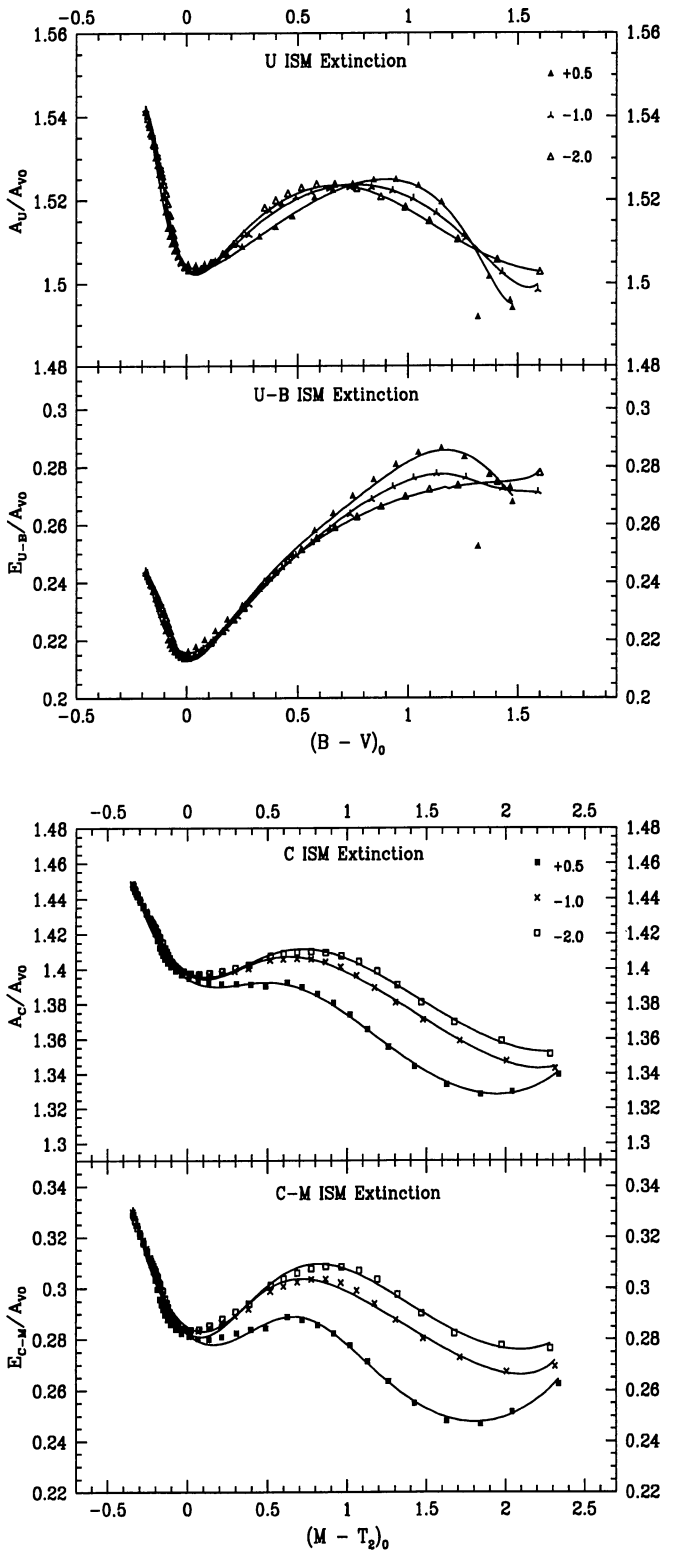

Fig. 5. a) and b) Same bands and colours as Fig. 4 for the three non-solar metallicities of the giants ($\log g$=2.5) alone. The code is [Fe/H]: solid, 0.5, skeletal, −1.0, hollow, −2.0. [Fe/H] = 0.0 has been displayed before. a) U, $U-B$, b) C, $C-M$

We see from the extinction curves of the giants in Fig. 5 that the $UBVRI$ extinctions in U and $U-B$ behave differently with abundance than do C and $C-M$. In the former the more metal rich population suffers less extinction in the cool stars, while for the Washington bands it is more. $C-M$ is somewhat more regular than $U-B$ for the more metal-rich population, and $M-T_1$ is much more regular than $B-V$ (Figs. 6 and 8).

The reduced extinction in $B-V$ for K giants and supergiants (Fig. 8) presents a problem for the determination of reddening and metallicity of reddened open clusters. If the colour dependent reddening correction to E_{B-V} is not applied, the cluster will dereddened too much in $B-V$, so that the distance and age may be underestimated, or serious errors made in the photometric measurement of metallicity.

The $B-R$ colour index is not often used, but it has considerable advantages over $B-V$ in the analysis of young clusters, showing emission stars clearly in young clusters that do not show up at all in $B-V$ (Grebel et al. 1994a), and serving as an index more sensitive to metallicity for the RGBs of older populations. In Fig. 7 we show the behaviour of this band and index.

In Fig. 9 we compare the colour dependent extinction behaviour of the best optical $UBVRI$ temperature colour $V-I$ and the Washinton temperature colour $M-T_2$.

To standardise a self-consistent internal reddening system comparable to that of UBV, we define a similar ratio to R_V for the Washington Canterna System,

$$R_{T2} = A_{T2}/E_{M-T2}.$$

In Fig. 10 we show these ratios for our usual set of luminosity classes and metallicities. These relations were quite difficult to fit with rational polynomials that did not have singularities in the colour domains.

The remainder of bands, RI and T_1T_2 have extinction behaviour well represented by straight lines.

We have plotted the U, $U-B$ extinctions versus $B-V$ and C, $C-M$ versus $M-T_2$ for reasons that were explained. But it is worthwhile to ask whether the extinction behaviour of these blue magnitudes would not be better if plotted against $U-B$ and $C-M$. We give such plots in Fig. 11. The improvement for C, $C-M$ appears significant, but note that for U, $U-B$, where the relation is double valued, the distribution is unimproved, and worst the hot main sequence stars follow a different relation. The surfave gravities of hot stars are not always easy to distinguish spectroscopically. *Determining the intrinsic U-B colour of a significantly reddened star is exceptionally difficult.*

4. Nonlinearities with A_V

Forbes (1842) observed that because the most extincted wavelengths are preferentially absorbed in an extended

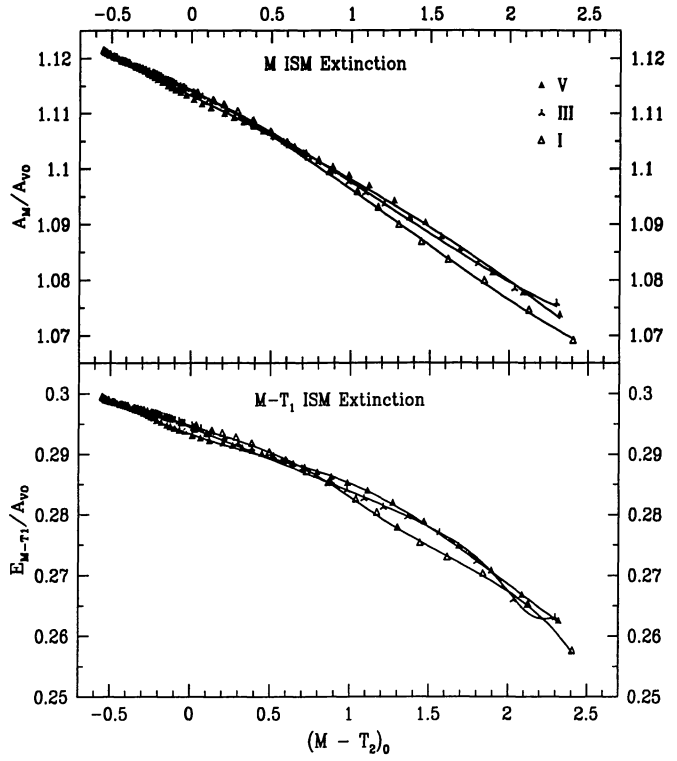

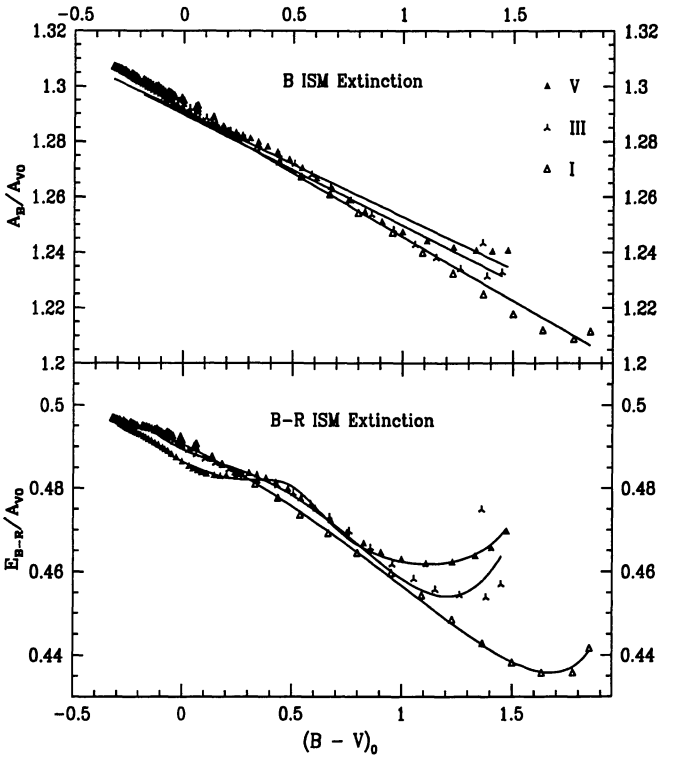

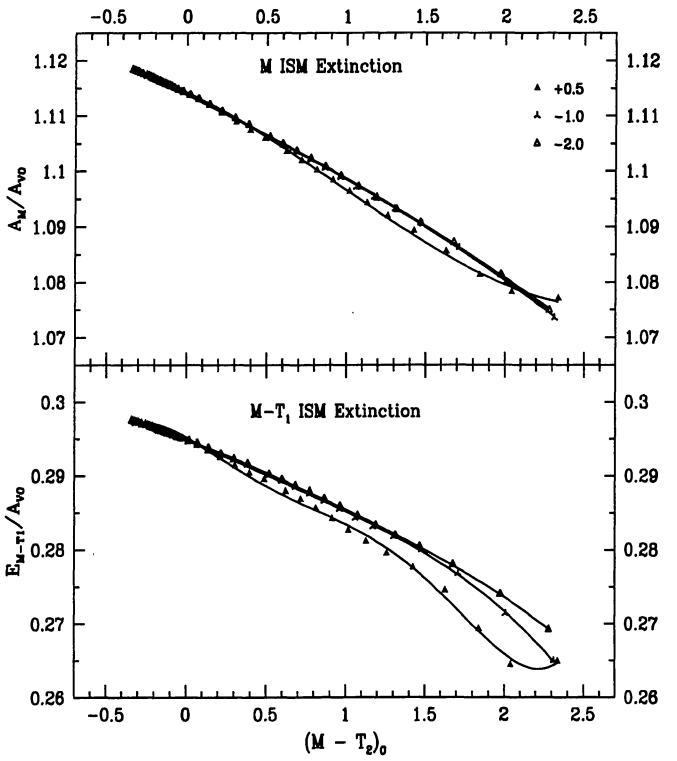

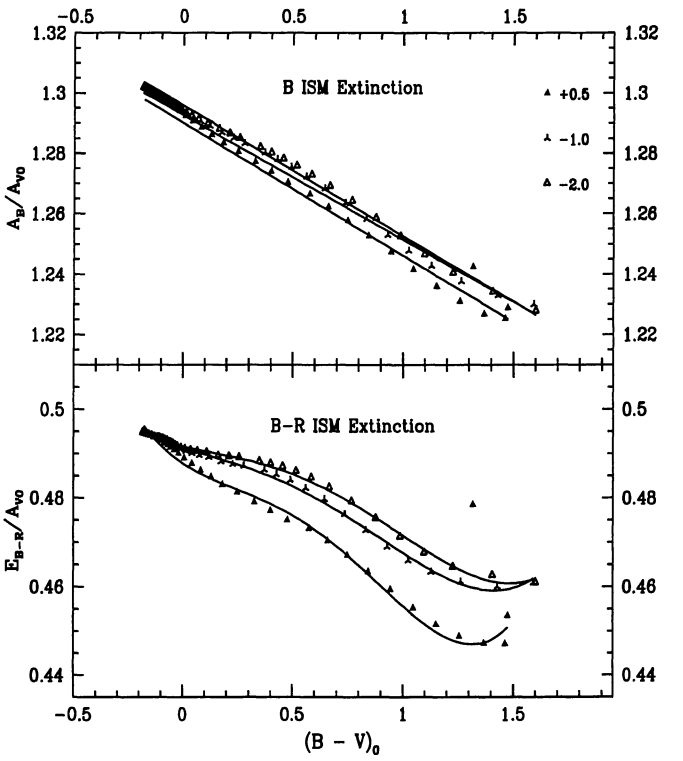

Fig. 6. a) and b) Combined relations of Figs. 4 and 5 for M, $M - T_1$: a) for the three surface gravities at solar metallicity, b) for the three metallicities of giants not presented in a)

Fig. 7. a) and b) Combined relations of Figs. 4 and 5 for B, $B - R$: a) for the three surface gravities at solar metallicity, b) for the three metallicities of giants not presented in a)

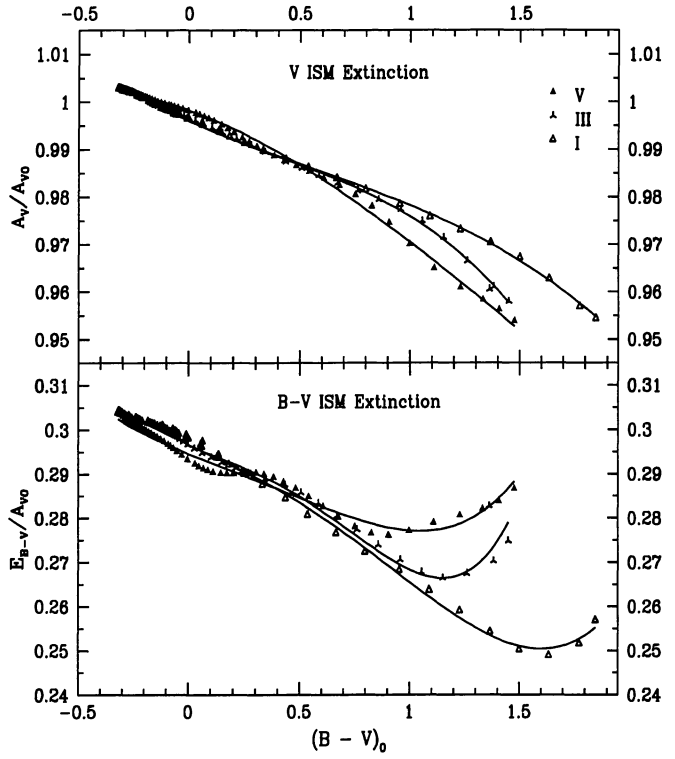

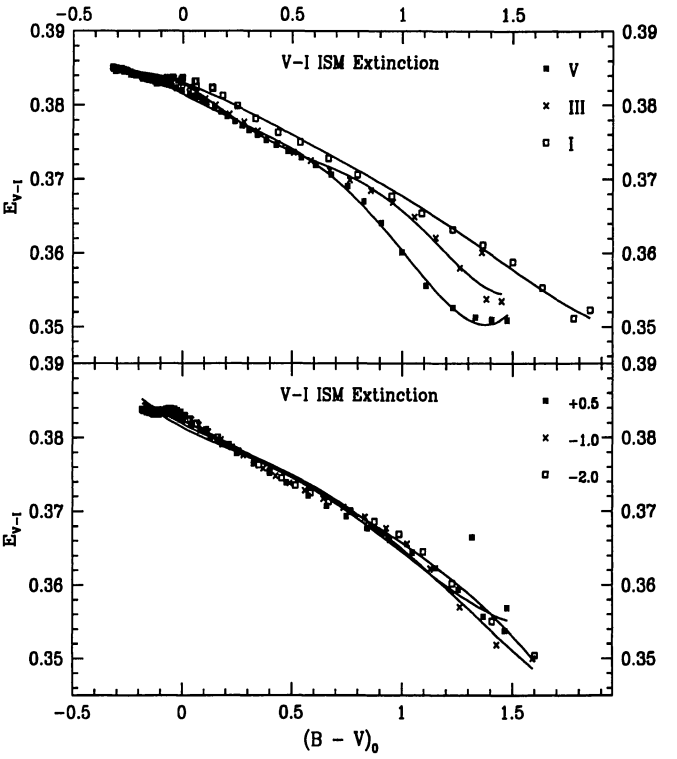

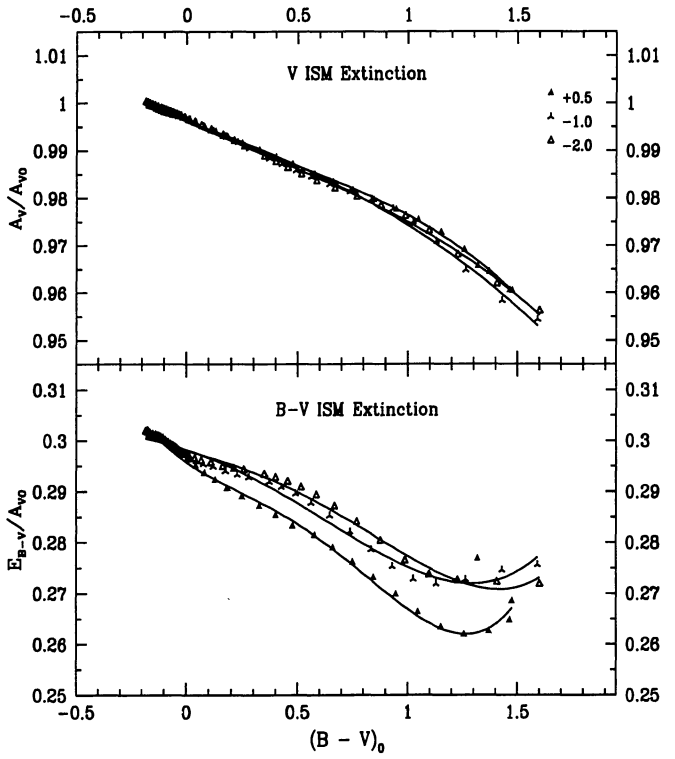

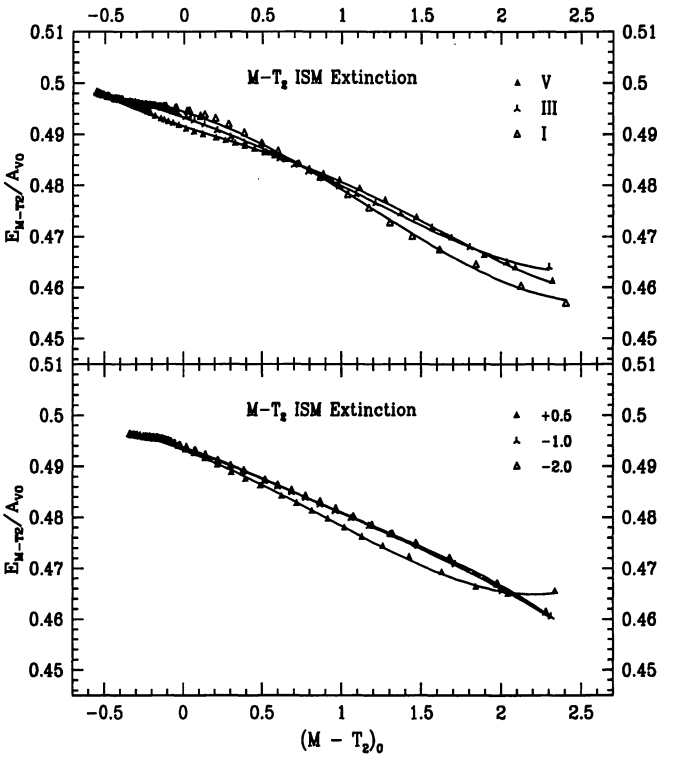

Fig. 8. a) and b) Combined relations of Figs. 4 and 5 for V, $B-V$: a) for the three surface gravities at solar metallicity, b) for the three metallicities of giants not presented in a)

Fig. 9. a) and b) Extinction behaviour for the temperature colours themselves. a) $UBVRI$ temperature colour $V-I$, b) Washington temperature colour $M-T_2$

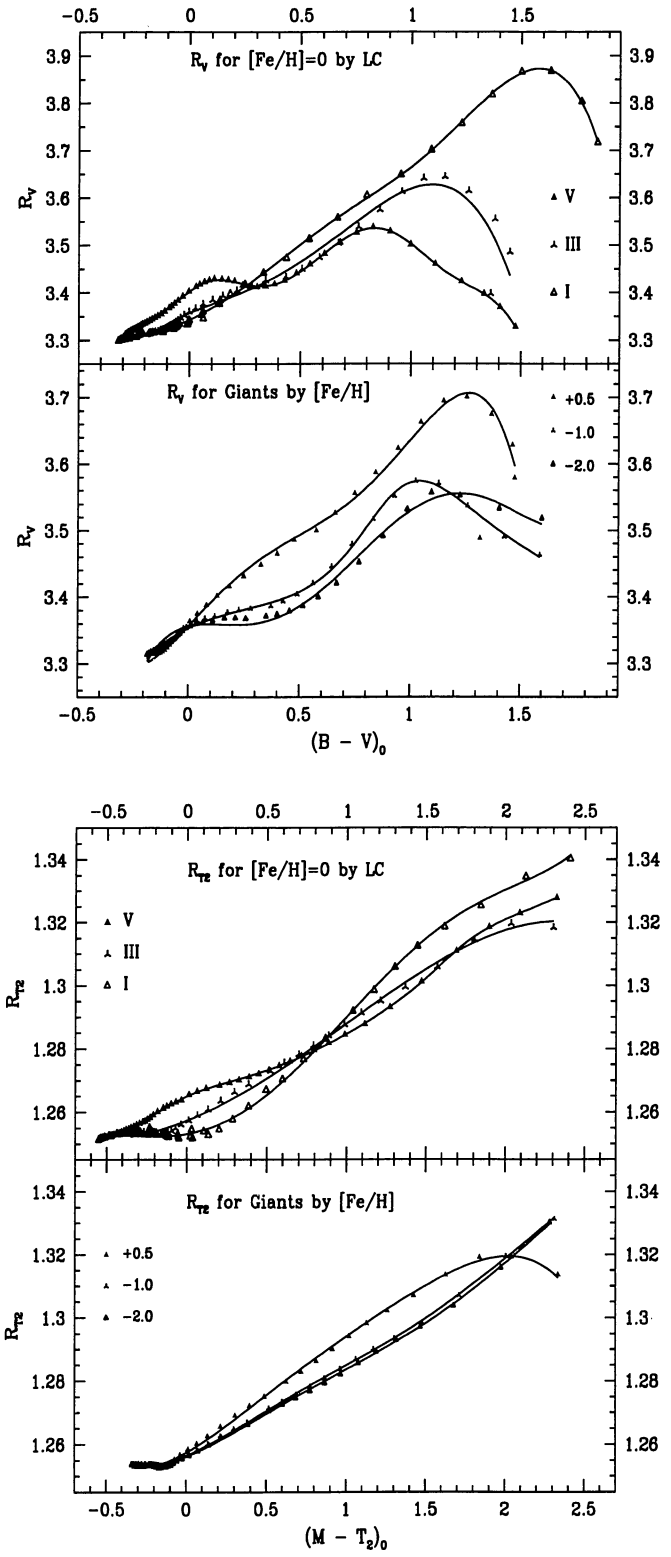

Fig. 10. a) and b) The ratios of total to selective extinctions. a) $R_V = A_V/E_{B-V}$, b) $R_2 = A_{T2}/E_{M-T2}$

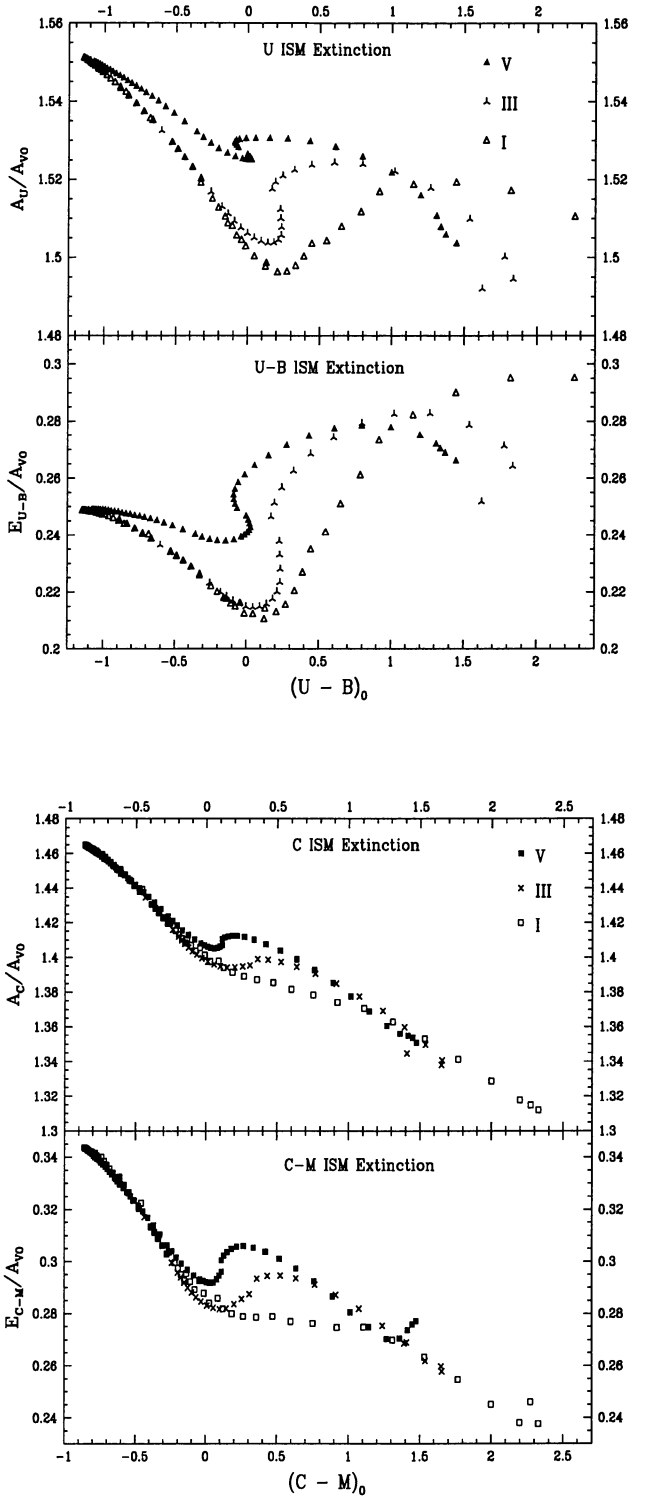

Fig. 11. Blue extinctions versus blue colours. Compare to Fig. 4 to see that there is no improvement in using $U-B$ as the transformation colour in reducing U and $U-B$, and little improvement in using $C-M$ as the transformation colour in reducing C and $C-M$. a) U & $U-B$ vs $U-B$, b) C & $C-M$ vs $C-M$

medium, the fractional absorption of a beam of light with an ensemble of wavelengths decreases as a light beam passes through an absorbing medium. Thus the absorption in the heterochromatic beam is not proportional to the quantity of absorbers traversed, that is, the absorption is nonlinear. He applied this reasoning to absorption in the atmosphere, but it applies also to interstellar space.

To evaluate the relative magnitude of the nonlinear heterochromatic extinction in interstellar space, we have evaluated the broadband extinction in each filter of the two systems in this paper at 25 multiples of the standard extinction curve, from 0.1 A_λ to 2.5 A_λ. In Fig. 12 we show the magnitude of the nonlinearity in each passband of both photometric systems by displaying the ratio of the cumulative extinction per unit A_V to the total extinction at $A_V = 1.0$. Because for any filter this function actually is different for every temperature, surface gravity, and metallicity, we assume solar metallicity and remove the temperature dependence by plotting the constant coefficient in a linear fit to the temperature colour, p_0 from Eq. (1). So we have in effect merely plotted the Forbes effect for stars whose temperature colour is 0.0 – approximately A0 stars.

In Fig. 12 we have plotted the three luminosity classes for solar metallicity, as in all previous plots. Obviously there is virtually no dependence of the Forbes effect on luminosity class. A similar plot of the other metallicites for the giants shows that there is no dependence on metallicity either.

Consider the C filter of the Washington system. Flux is removed from the light beam at a 0.3% greater rate at $A_{V,0} = 0.1$ than the cumulative rate for $A_{V,0} = 1.0$. So for small extinctions we should multiply A_C by 1.003. Clearly such a correction is negligible compared to other uncertainties involved. Even an absorption of 2.5 mag provides only 0.5% deviation from the linear result.

It might be expected that the U filter, being bluer, would exhibit a larger Forbes effect than the C filter. However, it is much narrower than C, and that is the crucial parameter. Its Forbes effect is only half as big as that for C. B is a wider filter more comparable to C, and it exhibits a Forbes effect almost as large. We see also that the Forbes effects for V and R are equally large, because they are broad, but in neither case is it significant, nor is it significant for the redder filters.

5. Applications

We will discuss only a few of the many possible applications of these derived Wildey extinctions. We have provided the necessary relations for a complete and accurate dereddening of all solar metallicity stars in these optical bands, and for giants and supergiants at three other metallicities that span all practical conditions.

These results also clarify the use of R_V and R_{T2} for characterizing the properties of interstellar dust, demonstrating that the R_V or R_{T2} found for a particular stellar

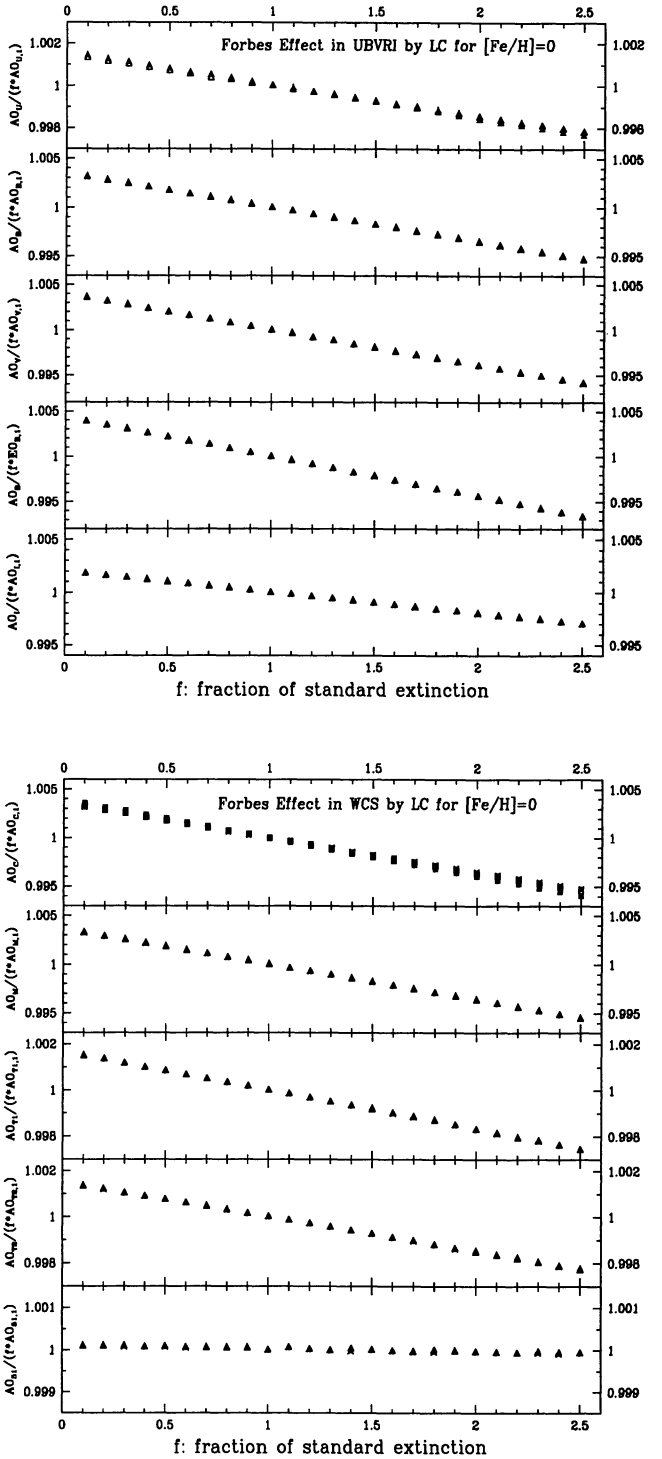

Fig. 12. a) and b) The Forbes effect – nonlinear heterochromatic extinction – for ISM extinction by luminosity class at solar metallicity. The plotted function is the ratio of the constant coefficient in the linear fit of the actual extinction to temperature colour, $A0_{M,f}$, to that at $A_{V,0}=f$, that is, $A0_{M,f}/(f \times A0_{M,1})$, a) $UBVRI$ system, b) Washington system. The narrow band dwarf discriminator DDO 51 shows almost no Forbes nonlinearity, as expected

probe must always be transformed to the standard spectrum before being compared to that found from other stellar probes.

The dereddening in the $U-B$, $B-V$ two colour diagram (TCD) is usually done by assuming a slope of $E_{U-B}/E_{B-V} \simeq 0.72-0.76$ independent of height in the diagram. More sophisticated treatments like that of Wildey (1963) permit the slope to change with increasing reddening owing to the increasing redward monochromaticity caused by the reddening. However, we have shown that this method may lead to error, because the slope varies with $U-B$ as we go up the main sequence.

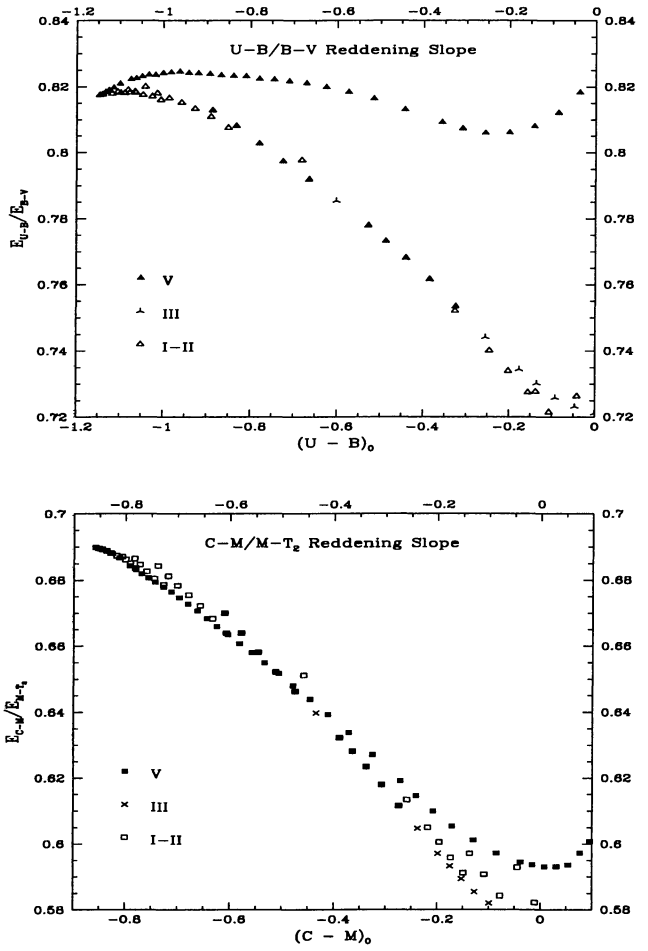

Fig. 13. a) and b) The reddening slopes for upper main sequence stars of solar metallicity, in the TCDs used for dereddening of hot stars as a function of the vertical colour. a) E_{U-B}/E_{B-V}, b) E_{C-M}/E_{M-T2}

In Fig. 13 we see influence of gravity and temperature on the dependence of the reddening slope on $(U-B)_0$. Only solar metallicity is shown. The radically differing behaviour of MS stars from the evolved stars is quite surprising. Clearly one must be very careful to know which type of star one is dealing with. An additional point is that in dereddening to the main sequence one must use a steeper slope than has been customary heretofore.

In the WCS the behaviour of the reddening slope is better in every way. The slope increases monotonically from 0.58–0.59 for A0 up to 0.69 for O3, and the slope does not depend on the luminosity class anywhere in the region of interest for OB stars.

We plot the actual reddening vectors in $B-V$, $U-B$ for dwarfs and giants at solar metallicity in Fig. 14. Because we are assuming $A_{V,0}$=1.0, we do not compute a reddening trajectory but merely the displacement vector. The actual trajectory is only very slightly curved (Wildey 1963), as we explained in Sect. 4.

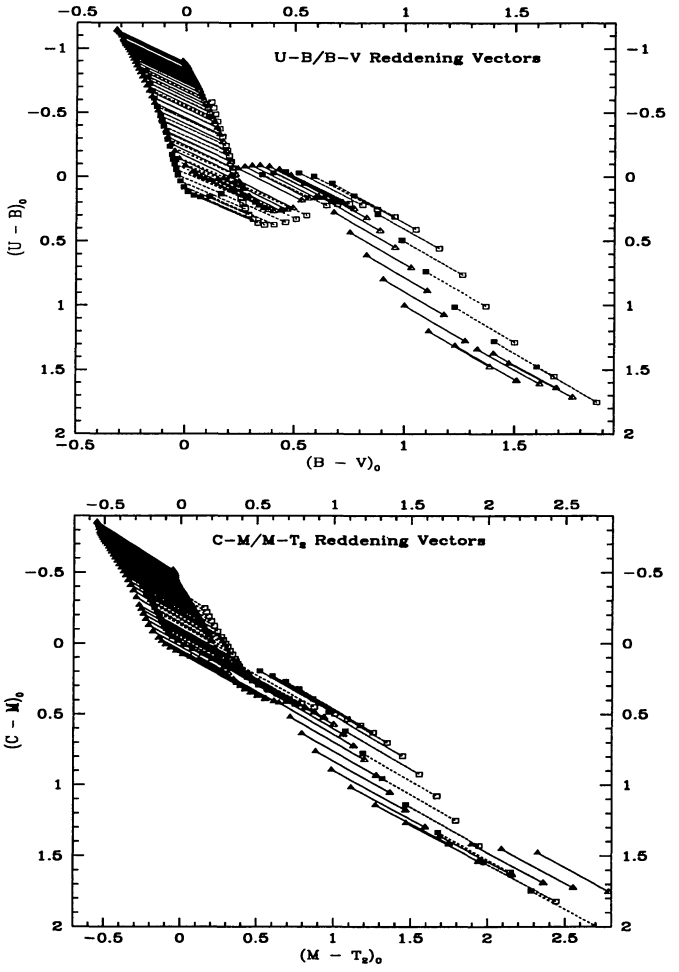

Fig. 14. a) The $UBVRI$ reddening vectors assuming a total reddening of $A_{V,0}$. Main sequence stars of solar metallicity are plotted with triangles and solid vectors. Giants with [Fe/H] = −2.0 are plotted with squares and dotted lines, b) The Washington reddening vectors assuming a total reddening of $A_{V,0}$. Main sequence stars of solar metallicity are plotted with triangles and solid vectors. Giants with [Fe/H] = −2.0 are plotted with squares and dotted lines

In the $(M-T_2, C-M)$ TCD (Fig. 14) the amount of reddening increases steadily all the way to the top. Thus a correctly dereddened upper MS is bluer and not as steep as that obtained when one incorrectly dereddens all the hot stars alike. Supergiants always have a unique dereddening solution in this diagram. It is clear that dereddening in Washington has advantages over that in UBV for hot stars as well as cool. Primarily the advantages are conferred by the gravity independence of the Washington slope and the more monotonic behaviour of $C-M$ in both reddening slope and with respect to temperature.

The reddening vectors we compute in the $(V-I, B-V)$ plane, shown in Fig. 15, are too parallel to the upper MS to be of much use, as is well known. However, in the $M-T_1$, T_1-T_2 plane they intersect at a greater angle *but from below*. The fact that these reddening vectors are blueward of the main sequence might be useful in bracketing the magnitude of the reddening of individual stars, but as far as we know such a method has never been tried.

The authors have applied these reddening results in their isochrone rating calculation in both *UBVRI* and Washington to young clusters in the Magellanic Clouds, and in Washington to the RGBs of the dSph galaxies Fornax and Sculptor (Grebel et al. 1994a,b,c,d). Our technique requires a correct treatment of the colour dependence of reddening in order to obtain results as accurate as they are precise.

6. Discussion

Following Wildey's (1963) pioneering work, we have shown that the colour dependence of interstellar extinction in blue broadband filters is a complicated function of the temperature, luminosity, and metallicity of the stellar probe. Even properties generally believed to be purely intrinsic to the properties of the dust, such as R, turn out to have a substantial dependence also on the properties of the stellar probe. Hence the measurement of all such extinction properties of the dust should be referred to the standard spectrum we have chosen: $T_{\rm eff} = 17\,000$ K, $\log g$=5.0, and [Fe/H] = 0.0, that is, a B3–5 star of solar metallicity on the main sequence. The tables presented in this paper make this transformation straightforward for the mean extinction law assumed.

Those who wish to merely use the linear part of the various fits to Eq. (1) can use $P_1(x) = p_0 + (p_1 - p_0 q_1)x$, which can be verified easily by direct division. Alternatively, one can use the purely linear fits from Table 5.

We have taken a conceptually simple phenomenological approach to the determination of reddening behaviour, which gives us great freedom to present the reddening for what it is, and to find the most compact formulas for it, without being limited by theoretical considerations. Our relations permit the accurate dereddening in any filter or colour of the *UBVRI* and Washington systems, provided that the average interstellar extinction law is obeyed.

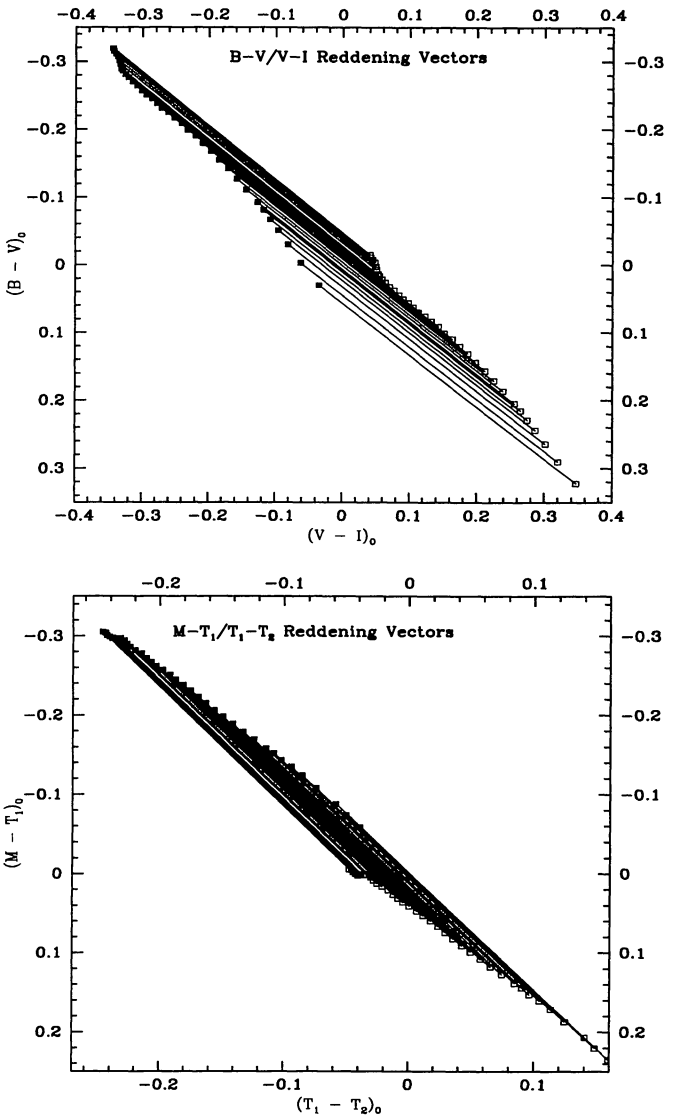

Fig. 15. a) and b) Reddening vectors for the next redder colour indices for the upper main sequence at solar metallicity. a) Note the well known property of the near parallelism of the vectors to the main sequence. b) The Washington vectors are only slightly more useful, but have the interesting property of having a *greater* slope than the main sequence; this property might be useful when combined with the vectors in the standard diagram

Our *method*, though, is completely general, and can be applied to any extinction law or filter system. We plan to extend it to the HST WFPC2 and FOC filter systems in the UV, using the new UV extinction law derived by Calzetti et al. (1994).

We show that the Washington system is superior to the *UBVRI* system in several important features useful for the measurement of interstellar reddening and determining the intrinsic properties of interstellar dust. We es-

Table 5. The coefficients of fits purely linear in temperature colour to the interstellar extinctions for all passbands considered in this paper

[Fe/H] =	+0.5		+0.0		-1.0		-2.0	
Band	a_0	a_1	a_0	a_1	a_0	a_1	a_0	a_1
A_U	1.520	-0.1074E-01	1.521	-0.1111E-01	1.520	-0.7863E-02	1.520	-0.7294E-02
A_B	1.294	-0.4213E-01	1.295	-0.3938E-01	1.297	-0.3709E-01	1.298	-0.3683E-01
A_V	0.997	-0.2056E-01	0.998	-0.2107E-01	0.998	-0.2073E-01	0.998	-0.2027E-01
A_R	0.805	-0.1810E-01	0.804	-0.1784E-01	0.804	-0.1841E-01	0.804	-0.1999E-01
A_I	0.615	-0.5536E-02	0.615	-0.5444E-02	0.615	-0.4726E-02	0.615	-0.4806E-02
A_C	1.412	-0.4033E-01	1.415	-0.3640E-01	1.417	-0.2954E-01	1.417	-0.2548E-01
A_M	1.114	-0.1653E-01	1.114	-0.1601E-01	1.114	-0.1561E-01	1.114	-0.1600E-01
A_{T1}	0.819	-0.4107E-02	0.819	-0.4297E-02	0.819	-0.5206E-02	0.819	-0.5952E-02
A_{T2}	0.621	-0.3057E-02	0.621	-0.3191E-02	0.621	-0.3011E-02	0.621	-0.3164E-02

tablish an internal reddening convention in the Washington system superior to the A_V, E_{B-V} convention in the $UBVRI$ system.

Finally, we give what is probably the single most used prescription in interstellar reddening – the correct colour-dependent reddening vectors for the standard extinction law on the upper main sequence in both the $UBVRI$ and Washington broadband photometric systems.

All colour dependent extinctions and their fit coefficients for main sequence stars, giants, and supergiants at [Fe/H] = 0.5, 0.0, −1.0, and −2.0 dex in the $UBVRI$ and Washington filters are available from the SIMBAD database (CDS) by anonymous ftp.

Acknowledgements. We thank H. Payne, D. Jones, and D.J. MacConnell for their assistance, R. Kurucz for his flux tables, and M. Bessell for his $UBVRI(+JHKK'LL')$ passbands. We thank A.T. Young for enlightening discussions, and A.W.J. Cousins and B. Baschek for useful criticism. E.K.G. was supported by an ESO student fellowship during most of this work, and also gratefully acknowledges the hospitality and support of the collaborative visitor program of the Space Telescope Science Institute, where much of this work was done. Almost all our programs use routines, many modified, from Press et al. (1992), copyright Numerical Recipes Software, Cambridge, MA.

References

Bell R.A., Paltoglou G., Tripicco M.J. 1994, MNRAS 268, 771
Bessell M.S. 1992, private communication
Blanco V.M. 1956, ApJ 123, 64
Blanco V.M. 1957, ApJ 125, 209
Buser R. 1978, A&A 62, 411
Buser R., Kurucz R.L. 1992, A&A 264, 557
Calzetti D., Kinney A.L., Storchi-Bergmann T. 1994, ApJ 429, 582
Canterna R. 1976, AJ 81, 228
Canterna R., Harris H.C. 1979, in Problems of Calibration of Multicolour Photometric Systems, Dudley Obs. Report No. 14, ed. A.G.D. Philip, 199
Cardelli J.A., Clayton G.C., Mathis J.S. 1988, ApJ 329, L23
Cardelli J.A., Clayton G.C., Mathis J.S. 1989, ApJ 345, 245
Crawford D.L., Mandwewala N. 1976, PASP 88, 917
Forbes J.D. 1842, Phil. Trans. 132, 225
Geisler D., Clariá J.J., Minniti D. 1991, AJ 102, 1936
Golay M. 1974, Introduction to Astronomical Photometry (D. Reidel, Dordrecht)
Gould A. 1994, ApJ 426, 542
Grebel E.K., Roberts W.J. 1994, A&A, in preparation (simultaneous isochrone rating)
Grebel E.K., Roberts W.J., Will J.-M., de Boer K.S. 1994a, Space Sci. Rev. 66, 65
Grebel E.K., Roberts W.J., van de Rydt F. 1994b in "The Local Group", 3rd CTIO/ESO Workshop, to be published
Grebel E.K., Roberts W.J., van de Rydt F. 1994c, A&A, submitted (Sculptor)
Grebel E.K., Roberts W.J., van de Rydt F. 1994d, A&A, submitted (Fornax)
Hill G. 1982, Pub. DAO 16, 67
Hiltner W.A., Johnson H.L. 1956, ApJ 124, 367
Kreĺowski J., Papaj J. 1993, PASP 105, 1209
Manfroid J., Sterken Chr. 1992, A&A 258, 600
Mathis J.S. 1990, ARA&A 28, 37
Paltoglou G., Bell R.A. 1994, MNRAS 268, 793
Press W.H., Teukolsky S.A., Vetterling W.T., Flannery B.P. 1992, Numerical Recipes in FORTRAN, 2nd Ed. (Cambridge Univ. Press, New York) (NR)
Roberts W.J., Grebel E.K. 1995a, A&AS, in press (Paper II)
Roberts W.J., Grebel E.K. 1995b, A&A, in preparation (validation of colours)
Scheffler H. 1982, Landolt-Börnstein Vol. 2c, Interstellar Matter; Galaxy; Universe (Springer-Verlag, Berlin) 46
Sterken C., Manfroid J. 1992, Astronomical Photometry, A Guide (Klewer Academic Publishers, Dordrecht)
Wildey R.L. 1963, AJ 68, 190
Young A.T. 1992a, A&A 257, 366
Young A.T. 1992b, in Automated Telescopes for Photometry and Imaging, ASP Conference Series, Vol. 28, 73
Young A.T. 1994, A&AS, in press (Improvements to photometry VI. Passbands and transformations)